Validation of an Enhanced Drinking Water Temperature Model during Distribution

Blokker, Mirjam; Pan, Quan; van Laarhoven, Karel

Important note
To cite this publication, please use the final published version (if applicable).
Please check the document version above.

Validation of an Enhanced Drinking Water Temperature Model during Distribution

Mirjam Blokker [1,2,*] [ID], **Quan Pan** [1] **and Karel van Laarhoven** [1] [ID]

1   KWR Water Research Institute, 3430 BB Nieuwegein, The Netherlands; karel.van.laarhoven@kwrwater.nl (K.v.L.)

2   Water Management, Civil Engineering and Geoscienses, Delft University of Technology, 2628 CN Delft, The Netherlands

*   Correspondence: mirjam.blokker@kwrwater.nl; Tel.: +31-306069533

Abstract: Drinking water temperatures are expected to increase in the Netherlands due to climate change and the installation of district heating networks as part of the energy transition. To determine effective measures to prevent undesirable temperature increases in drinking water, a model was developed. This model describes the temperature in the drinking water distribution network as a result of the transfer of heat from the climate and above and underground heat sources through the soil. The model consists of two coupled applications. The extended soil temperature model (STM+) describes the soil temperatures using a two-dimensional finite element method that includes a drinking water pipe and two hot water pipes coupled with a micrometeorology model. The extended water temperature model (WTM+) describes the drinking water temperature as a function of the surrounding soil temperature (the boundary temperature resulting from the STM+), the thermal sphere of influence where the drinking water temperature influences the soil temperature, and the hydraulics in the drinking water network. Both models are validated with field measurements. This study describes the WTM+. Previous models did not consider the cooling effect of the drinking water on the surrounding soil, which led to an overestimation of the boundary temperature and how quickly the drinking water temperature reaches this boundary temperature. The field measurements show the improved accuracy of the WTM+ when considering one to two times the radius of the drinking water pipe as the thermal sphere of influence around the pipe.

Keywords: drinking water temperature; water quality; model validation

1. Introduction

During transport and distribution, drinking water temperature can increase because of the relatively high temperatures of soil surrounding drinking water distribution networks (DWDNs). Temperature is especially relevant to the microbial quality of drinking water in a DWDN [1,2]. A drinking water temperature below 25 °C at the tap is required to meet Legionella prevention and/or drinking water standards [3]. Soil temperatures are affected by climatic factors and anthropogenic heat sources above and below ground level [4,5]. With climate change, urbanization, and the energy transition, which—in the Netherlands, in particular—comes with an expected increased number of district heating networks (DHNs), urban subsurfaces will heat up even further. Currently, the drinking water temperature at the tap sporadically exceeds the norm, but, with these developments, more exceedances are expected [3].

As pipes in a DWDN can typically last for more than 100 years and modifications during their lifetimes are expensive, measures to prevent high drinking water temperatures should be taken in the coming years, well in advance of temperatures rising to problematic levels. To understand the effectiveness of various measures to keep drinking water temperature at the tap below the threshold, a modeling approach is followed. Such a model requires the

possibility of modeling a highly meshed DWDN (a) in which the flows are constantly changing; (b) with various boundary conditions of the produced (incoming) drinking water temperature, which depend on the season; (c) with various boundary conditions of the soil temperature around the DWDN, which depend on the season and underground heat sources, such as the DHN; and (d) that leads to an accurate simulation of drinking water temperatures, thus allowing for the determination of effective measures to keep the drinking water temperature below the threshold of 25 °C. Blokker and Pieterse-Quirijns [4] developed an approach with a one-dimensional soil temperature model (STM) and a drinking water temperature model (WTM). The WTM calculates the drinking water temperature at each customer's location based on a hydraulic network model (requirement a) and heat exchange between the soil around the pipe wall and the drinking water (requirement b), where the soil temperature is calculated by the STM. The STM was first developed (and validated) for soil temperatures in shallow underground, urban environments (i.e., in sand and under tiles). It was then expanded to include weather forecasts [6], other soil types (peat and clays, with their specific heat exchange properties), other soil covers (grass and trees), and generic anthropogenic heat sources [5]. The STM does not allow for modeling a specific anthropogenic heat source, such as a DHN (requirement c). The WTM was validated in a DWDN at locations with long residence times, allowing for validation of the temperature of drinking water reaching the soil temperature but not the rate at which this happens. Therefore, it is unclear if temperatures in the entire DWDN are determined accurately (requirement d). When one wants to estimate the importance of specific influences on the drinking water temperature (e.g., climate change, DHN, or countermeasures), it becomes important to validate the WTM over its temporal scale.

The WTM assumes a constant temperature at the outer pipe wall, disregarding that—in reality—heat exchange between the drinking water and the soil also affects the soil temperature within a certain sphere of influence. Various authors have suggested adding an insulation layer of soil around the DWDN in a WTM-like approach [7–9]. Each suggested a different approach to determine the insulation layer's thickness. The validity of their approaches is unclear, as two [7,9] were only theoretical. The third [8] validated the model against measured water temperatures. Still, as the model included heat loss at consumers' locations, the impact of the conductive and convective heat resistances of the soil is unclear. Hypolite et al. [10] showed that good estimates of drinking water temperature can be obtained for a system of large transport mains when the role of the soil in heat transport is considered. Models for water temperature in underground networks are also used to determine heat losses in a DHN [11–16]. For a DHN, a simple modeling approach without explicitly incorporating an insulation layer of soil around the network suffices. Firstly, the heat losses at the consumers' locations are more substantial than the heat loss in the network and, secondly, the temperature differences between the soil and the water in the DHN are large. In order to obtain a good estimate of the order of magnitude of the heat losses, the heat exchange with the soil does not need to be known with high accuracy.

The time it takes for the temperature of the soil around a drinking water main to change is in the order of days to weeks. The time it takes for the temperature of drinking water to change is in the order of minutes to hours. As these temporal scales differ significantly, the approach of two models was used. Both models were improved, leading to (1) an enhanced STM called STM+ [17], which calculates the soil temperature profile, as it is influenced by both drinking water temperatures and external influences, such as the DHN and the weather; (2) an enhanced WTM (called WTM+), which calculates the drinking water temperature, as it is influenced by the soil temperature, as calculated by the STM+. The time scale of the WTM+ is typically hours; the time scale of the STM+ is typically months. The result of the STM+ is a soil temperature used as a boundary condition by the WTM+.

The STM+ is described and validated; the reader is referred to van Esch [17]. In the present paper, we describe the WTM+, in particular, how the thermal sphere of influence is modeled. To show that the WTM+ has improved with respect to the WTM, proper validation is essential. We validate the model with two cases. The first case is a single pipe

of ca. 1 km long with a variation in residence times. The second case is a DWDN, where half of the network is potentially influenced by a DHN, and the other half is not.

2. Materials and Methods

2.1. The Water Temperature Model (WTM+)

The change in water temperature, T_{water}, due to heat transfer (during contact time t) between the surroundings and the flowing water in a pipe can be described as follows [4,18]:

$$\frac{dT_{water}}{d\tau} = k\left(T_{boundary} - T_{water}\right) \quad (1)$$

where $T_{boundary}$ is the temperature that the drinking water will eventually reach and k is the heat transfer rate (1/s). In the modeled system, $T_{boundary}$ is assumed to occur at some distance from the pipe wall (Section 2.2 discusses how to determine $T_{boundary}$) and k depends on that distance and the characteristics of the water, pipe material, pipe surroundings, and the hydraulic characteristics of the water flow. Specifically, k is given by the following [4,18]:

$$k = \frac{4 \cdot \alpha_{water}}{D_1^2 \left(\frac{1}{Nu} + \frac{\lambda_{water} \cdot In\left(\frac{D_2}{D_1}\right)}{2\lambda_{pipe}} + \frac{\lambda_{water} \cdot In\left(\frac{D_3}{D_2}\right)}{2\lambda_{soil}} \right)} \quad (2)$$

where D_1 is the inner pipe diameter (m), D_2 is the outer pipe diameter (m), and D_3 is the diameter where the boundary condition $T = T_{boundary}$ is applied (m). The dimensionless Nusselt number, Nu, summarizes the hydraulic conditions of the system and—for pipes—can be described as a function of the dimensionless Reynolds number (Re) and Prandtl number (Pr): $Nu = 0.027\, Re^{0.8}\, Pr^{0.33}$ for turbulent flows ($Re > 10000$) and $Nu = 3.66$ for laminar flows ($Re < 2300$). Furthermore, α_{water} is the thermal diffusion coefficient [0.14×10^{-6} m^2/s]; $\alpha_{water} = \lambda_{water}/\rho_{water}\, C_{p,water}$; λ_{water} is the thermal conductivity of water [0.57 W·m^{-1}·K^{-1}]; ρ_{water} is the density of water [1000 kg·m^{-3}]; $C_{p,water}$ is the heat capacity of water [4.19×10^3 J·kg^{-1}·K^{-1}], with the parameter values given at 20 °C. In this paper, we only consider plastic pipes, for which λ_{pipe} is the thermal conductivity of PVC [=0.16 W·m^{-1}·K^{-1}]. We typically consider pipes that are installed in sand, for which λ_{soil} is the thermal conductivity of dry, sandy soil [=1.6 W·m^{-1}·K^{-1}].

With the time-dependent boundary conditions $T_{water}(\tau = 0) = T_{water,0}$ and $T(\tau = \infty) = T_{boundary}$, the analytical solution is as follows:

$$T_{water}(t, \tau) = T_{boundary}(t) + \left(T_{water,0}(t) - T_{boundary}(t)\right)exp(-k\tau(t)) \quad (3)$$

where t is time and τ is the contact time (in the drinking water context, this is the residence time). It is important to note that k can also be time-dependent, e.g., when hydraulic conditions change over time. Equation (1) to Equation (3) derive from Fourier's heat equation, describing how T_{water} changes over time during transport through the network, with the local difference between T_{water} and $T_{boundary}$ as the driving force for local heat transfer. A central assumption is that the temperature profiles in the pipe wall and the surrounding soil are developed into a steady state. This assumption is reasonable if the drinking water temperature changes much faster than the soil temperature profiles.

Figure 1 visualizes how the equations and boundary conditions of the current model (Figure 1b,c) and those of its predecessor (Figure 1a) approximate the temperature profile in the modeled system. Figure 1a (the left panel) shows the situation modeled by the original WTM, where a constant soil temperature is applied directly onto the outer pipe wall (green dot), i.e., $R_3 = R_2$. No gradient in the soil temperature profile is considered.
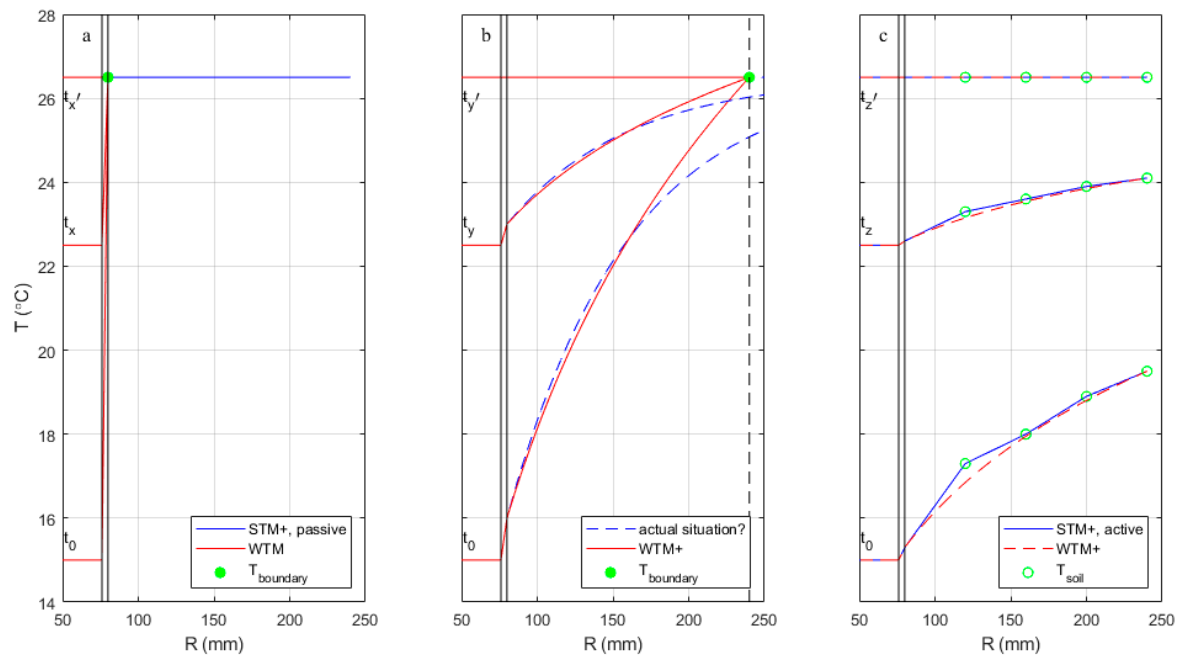
Figure 1. A schematic view of the water and surrounding soil temperature versus the distance R from the pipe center for a Ø160 mm PVC pipe. On the left (**a**) is the old model approach with STM and WTM, where the soil has an infinite heat capacity. On the right (**c**) is the model approach with STM+, with a fitted WTM+, where the drinking water has an infinite heat capacity. In the middle (**b**) is a hypothesized actual situation where the soil and drinking water temperature affect each other. The red lines describe the WTM(+) for three values of T_{water} (15, 22.5, and 26.5 °C). The time it takes to move from one situation to the next differs in the three modeling approaches, indicated as t_x, t_y, t_z, and t_x', t_y', t_z'. The green dots indicate the coupling between WTM+ and STM+ both in the distance from the pipe wall (R_3) and temperature value ($T_{boundary}$). The solid blue line (right) shows the STM(+) result, as taken from Figure 6.10 in the work by van Esch [17].

Figure 1c (the right panel) shows one first possible approximation of the presented approach. When heat is exchanged between soil and water, a soil temperature profile develops with a gradient that attenuates with increasing distance from the pipe. The blue lines and green dots show the profile that develops around a pipe in which the water temperature is kept constant for a long time, as modeled with the STM+. This profile could be used as input for the WTM+ by using the T_{soil} and R of any green dots to determine $T_{boundary}$ and D_3 (dotted red lines). If a $T_{boundary}$ of 26.5 °C is used, like in the other panels, that requires a D_3 corresponding to an R of approximately 1400 m.

Figure 1b (the center panel) shows a presumably more realistic approximation of the presented approach. Contrary to the assumptions of the previous two figures, the temperatures of both the water and the pipe surroundings may change over time at any one specific location along the network. As a result, it is unrealistic to expect the fully developed temperature profiles of Figure 1c. Instead, a dynamic profile between fluctuating soil and water temperatures should be expected, represented by the dotted blue lines. If a semi-steady state can be assumed for this profile, it could be modeled with WTM+ by applying the temperature $T_{boundary}$ at some distance R_3 (the radius corresponding to D_3 in the equations) of the pipe (green dot) in a way that the slope of the profile is best approximated. The true temperature profile will not be discontinuous at R_3, so the temperature profile that follows from Equation (1) to Equation (3) (red lines) does not perfectly describe the realistic situation.

In each panel of Figure 1, the model behavior is shown for three different values of T_{water}. These three temperatures can be imagined as occurring over the length of the pipe as the drinking water travels through the network. This means that, after a certain time t, the

drinking water will have traveled a certain distance x, and the drinking water temperature will then have increased under the influence of $T_{boundary}$ assumed for the surrounding soil (26.5 °C in this example). For Figure 1a, the temperature gradient for any given water temperature is much steeper (and thus heat exchange is faster) than for Figure 1b. The example temperatures will therefore be reached at different moments in time, which is why different suffixes are used to indicate the time. The situation in Figure 1a—the old WTM— will lead to an overestimation of how quickly drinking water will heat up compared to the actual situation because heat transfer is never decreased by the development of a less steep temperature gradient in the soil. The situation in Figure 1c will lead to an underestimation of how quickly drinking water will heat up compared to the actual situation because the exaggerated removal of heat for the soil by water with a constant temperature leads to overly attenuated temperature gradients and heat transfer in the soil.

Applying a $T_{boundary}$ at a distance D_3 in the WTM+ should be considered a mathematical approximation to compensate for the fact that we have not built one integrated model but two coupled models (WTM+ and STM+), while the boundary conditions of the two are not fully independent. Equation (2) assumes that D_3 is constant over time, and Equation (3) assumes that D_3 and $T_{boundary}$ are constant over the residence time t (i.e., constant over the pipe length). $T_{boundary}$ is determined with the STM+; see Section 2.2.

In practice, the value of D_3, the distance at which a constant $T_{boundary}$ can reasonably be applied, is not known a priori. In this study, we try to estimate the value of D_3 from measurements of T_{water} at various distances and residence times (t_0, t_y, t_y') and estimates of $T_{boundary}$ (using the STM+) in two case studies (Sections 3 and 4). Various authors [7–9] have suggested values for D_3 related to the pipe installation depth. However, it is unclear which approach works best, partly due to a lack of validation. We expect that the value of D_3 is most likely larger for large pipe diameters than for small pipe diameters, with a large body of water having more potential to influence the soil around the pipe. To make this scaling influence of the pipe diameter more explicit, we introduce the thermal sphere of influence (TSoI) as an explicit scaling factor: $D_3 = D_2 + 2 \times \text{TSoI} \times D_1$.

2.2. $T_{boundary}$ from the Soil Temperature Model (STM+)

$T_{boundary}$ in Equation (1) is the temperature that the drinking water will eventually reach, and this takes place when the soil and drinking water temperature are in an (dynamic) equilibrium. This equilibrium temperature ($T_{boundary}$) may differ from the undisturbed soil temperature and therefore is determined with the STM+. For a thorough description of the STM+, including its validation, the reader is referred to work by van Esch [17].

The STM+ input parameters are a time series of atmospheric circumstances (temperatures, radiation, etc., a so-called micrometeorology model), type of surface (tiles, grass, and trees), and type of soil (dry or wet sand and clay) and evaluate heat transfer for a 2-dimensional geometry, which includes a drinking water pipe. The STM+ calculates soil temperatures in a large grid around the drinking water pipe. The temperatures around the pipe are not constant. Instead, the average temperatures over the circumference of circles around the pipe wall (at a distance of one to two times D_2) were reported as relevant for determining $T_{boundary}$. The STM+ average temperature is referred to as "the" soil temperature at a certain distance from the pipe wall (T_{soil}).

The STM+ can be operated in the so-called "passive" and "active" modes. In the passive mode, the drinking water temperature is a simulation result and not a boundary condition, i.e., T_{soil} influences the drinking water temperature, but not vice versa. It was shown that T_{soil} is practically constant over the distance from the pipe wall (up to $3 \times D_2$, or TSoI = 0.2 to 1) and equal to the calculated T_{water}. This, by definition, is $T_{boundary}$. van Esch [17] showed that $T_{boundary}$ from the STM+ passive mode is equal to T_{soil} from the STM, so equal to the undisturbed soil temperature. It is important to note that this mode is used in the left panel of Figure 1. In the active mode, a constant drinking water temperature is imposed, which means that the drinking water acts as an infinite heat source. van Esch [17] showed that, in this case, T_{soil} can be described as a function of the distance from the pipe

wall (up to TSoI = 1) and $T_{water,0}$. In addition, $T_{boundary}$, defined as the temperature reached when the soil and drinking water temperature are balanced, can easily be determined and is practically independent of this distance from the pipe wall (up to TSoI = 1). This mode is used in the right panel of Figure 1.

This means that the STM (or STM+ passive mode) combined with the WTM (or WTM+ with $D_3 = D_2$) reflects the situation of stagnant drinking water. The STM+ active mode combined with the WTM+ reflects the situation where the drinking water at a certain location in the pipe is continuously refreshed and kept at a constant temperature, and there is an equilibrium with the soil temperature. This mimics water flowing at a constant flow rate, where the soil temperature along the pipe is constant. In a typical drinking water distribution main, the flow rate changes over the day with (almost) stagnant water during the night and high flow rates during peak hours. The conditions are, therefore, never equal to those in the passive or active mode. Furthermore, the two modes lead to a different value for $T_{boundary}$; van Esch [17] showed that, for summer conditions, the passive mode leads to a slightly higher value than the active mode. This means that, in the case studies in this study, the coupling between STM+ and WTM+ is not obvious, i.e., both D_3 and $T_{boundary}$ are unknown.

2.3. Model Normalization for Validation

In case study 1, the measurements are conducted over a few weeks, and the boundary conditions $T_{boundary}$ and $T_{water,0}$ are not constant over this period, with a maximum change of 1.0 °C per 24 h. We assume that k in Equation (3) is constant during each test at a specific (constant) flow rate and, from it, we want to determine the value for D_3. In order to achieve this, we rewrite Equation (3), assuming that, at each time t during each test, the equation is valid. The model is normalized across tests with $T_{water}(\tau) = T_{water,\,0} + \Delta TN \cdot \left(T_{boundary} - T_{water,\,0} \right)$ and $0 < \Delta TN < 1$:

$$\Delta TN(\tau, t) = 1 - exp(-k\tau(t)) = \frac{T_{water}(\tau, t) - T_{water,0}(t)}{T_{boundary}(t) - T_{water,0}(t)} \tag{4}$$

The normalized temperature difference ΔTN represents the change in the temperature of the drinking water along the pipe length relative to the difference in drinking water temperature and the surrounding soil, which we refer to as the driving force. The result is graphically shown in Figure 2 for various values of D_1 and D_3, where $\Delta TN = 0$ represents $T_{water}(\tau) = T_{water,0}$ and $\Delta TN = 1$ represents $T_{water}(\tau) = T_{boundary}$, even when the boundary conditions are not constant.
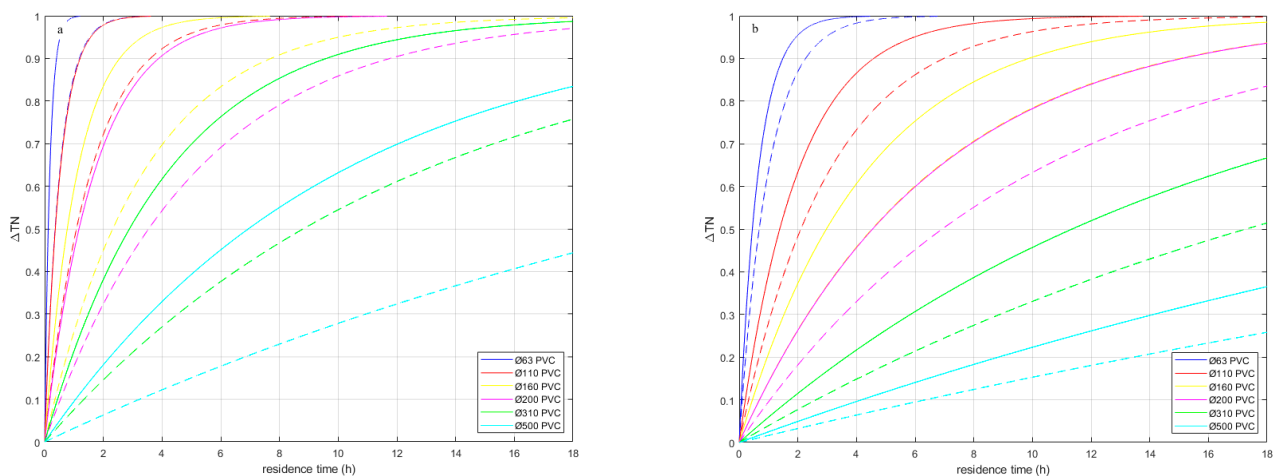
Figure 2. ΔTN versus the residence time for various diameters of PVC pipes with $D_3 = D_2$ (solid lines, TSoI = 0) and $D_3 = 3 \times D_1$ (dotted lines, TSoI $\approx$ 1). The legend indicates the nominal diameters of PVC pipes (D_2) (**a**) for turbulent flows ($Nu = 100$) and (**b**) for laminar flows ($Nu = 3.66$).

2.4. Case Studies

The validity of the approach of the WTM+ to model the drinking water temperature over the length of a pipe with $T_{boundary}$ from the STM+ and a layer of soil as an insulator (TSoI) needs to be verified. This will be achieved in two case studies: the first case study is a single pipe with an internal diameter of 152 mm and the second one is a DWDN, where most pipes have an internal diameter of 100 mm. Case study 1 had limited spatial variation, where many parameters were well defined but had significant temporal variation; case study 1 had limited temporal variation but significant spatial variation, with some unknown parameter values. As the value of the TSoI is not yet known, the case studies will also be used to estimate its value. This means that the case studies are used both for validation and calibration.

For both case studies, a sensitivity analysis was performed (reported in Appendices B.3 and C.3), and measurements were taken for validation and calibration. The details are described per case study.

2.5. Description Case Study 1—Single Pipe, Ø160 mm PVC

A 925 m long Ø160 mm PVC pipe (D_1 = 152 mm, D_2 = 160 mm) in Rotterdam with only a few connections along the pipe stretch was selected by Evides water company and KWR to validate the WTM+ (and the STM+). This pipe is fed from a surface water PS (pumping station) through 3 km of large-diameter mains (PVC internal diameter > 1350 mm) and a smaller branch of 570 m (internal diameter of 150.6 mm). It is assumed that the temperature at the start of this branch is equal to the temperature from the PS (ΔTN < 0.05 after 4 h for Nu = 100 (turbulent flow), PVC DN1400, and D_3 = 0). The end of this branch is the first location (L1) of the case study. The water in the case study pipe flows from location L1 to L2 (415 m) to L3 (510 m). For this pipe, taking the example of Figure 1, the required residence times (for turbulent flows) can be estimated as $t_x \approx 1$ h, $t_x' \approx 8$ h, $t_y \approx 3$ h, $t_y' \approx 24$ h, $t_z \approx 9$ h, $t_z' \approx 61$ h. This means that measurements are focused on the residence times between 1 and 24 h.

For the single pipe, a sensitivity analysis for ΔTN was performed analytically (see Appendix B.3). It shows that $\left(T_{boundary} - T_{water,0} \right)$ and λ_{soil} are the most influential parameters. There is a distinct difference between turbulent and laminar flows.

The drinking water temperature was measured at PS, L1, and L3, with a resolution of ± 0.1 °C. The flow between L1 and L3 was controlled with a hydrant at L3 and measured. During a two-week period (18 May 2020–3 June 2020), the flow rate was controlled such that residence times of the water in the pipe from 1 to 24 h were obtained (see Table A1). At the same time, soil temperatures were measured at various distances from the pipe wall at locations L1, L2, and L3, which were used to validate the STM+ [17]. The values for input parameters used in the WTM+ (Equations (2) and (4)) are shown in Table A2. Appendix B.1 has more information on the test location, including a schematic overview.

During the measurements, there was practically no demand from customers along the pipe, as there were only one residential customer and some sports facilities, which were closed during the COVID-19 pandemic. The demand at the customer location was measured, and it had a negligible effect on the flow at L1. The logging frequency for flow and temperature measurements was once per 15 min. The residence time between L1 and L3 was calculated from the pipe length, pipe diameter, and flow.

$T_{boundary}$ was estimated with the STM+ [17] results for L3, where detailed info on the actual soil parameters was used. The STM+ was validated in this particular case study, and then the model was rerun in the so-called passive mode and active mode (see Section 2.2), both for laminar and turbulent flows. $T_{boundary}$ for stagnant water (STM+ passive mode) was 0.3 to 0.9 (on average 0.7) °C lower than $T_{boundary}$ for turbulent flowing water (STM+ active mode, Nu = 3.66) and 0.2 to 0.7 (on average 0.5) °C lower than $T_{boundary}$ for laminar flowing water (STM+ active mode, Nu = 100).

During each test, the flow was kept constant. After a certain time (and with constant incoming drinking water temperatures), a dynamic equilibrium, as in the situation simulated in the STM+ active mode, could be expected. However, the constant flow was only

imposed for a relatively short time, viz. 5 h to max 66 h (Table A1), and the incoming water temperature was not constant. This means that it is not obvious which STM+ (passive or active mode for turbulent or laminar flows) would be applicable. The small differences in $T_{boundary}$ for this case study will have a significant effect because the difference between incoming and outgoing water temperatures and soil temperatures is relatively small (<2.0 °C). As it is unclear which is the "true" $T_{boundary}$, both STM+ modes are tested.

Data processing is required to validate the WMT+ with the measurements (Appendix B.2). A normalization step was performed because none of the parameters in Equation (4) are constant over time. Also, due to measurement accuracies, some data were excluded with the error estimation of Appendix A (22 data points where the drinking water temperature between the beginning and the end of the pipe seemed to change in the opposite direction compared to the soil temperature; 93 data points where the uncertainty was too large). As a last step, the individual data points with similar residence times were grouped and shown in boxplots.

2.6. Description Case Study 2—Drinking Water Distribution Network

Case study 2 for validating the WTM+ consisted of drinking water temperature measurements performed on 31 August 2020 in the DWDN of Almere. The Almere DWDN, owned and operated by Vitens, is ca. 700 km long and mainly consists of PVC pipes, with nominal diameters of Ø63 (8%), Ø110 (51%), Ø160 (15%), Ø200 (5%), Ø310 (6%), and > Ø400 mm (9%) (more info in [19]). The DWDN is fed by two feeding reservoirs in the northern and southern parts of the system, referred to as F1 and F2 (Figure 3). The drinking water temperature was $T_{water, F1}$ = 13.7 °C and $T_{water, F2}$ =13.3 °C on 31 August 2020, respectively. Limited variation in these temperatures is expected throughout the test (less than a day), as this is drinking water from a groundwater source.
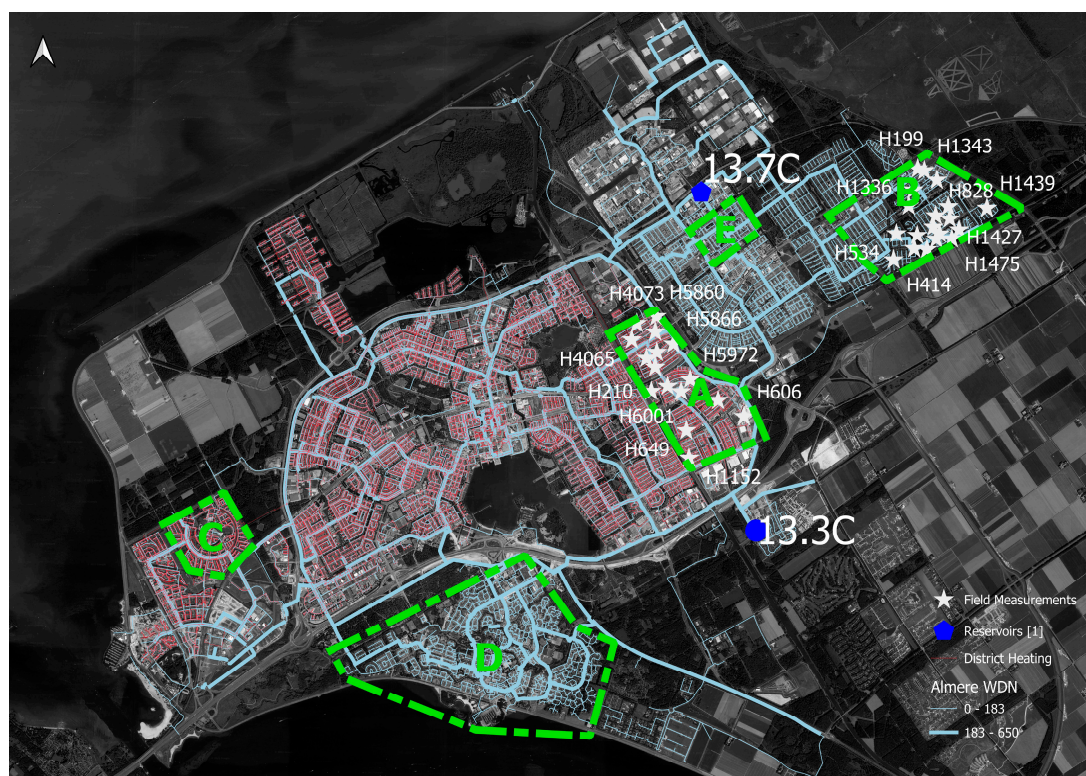
Figure 3. Almere reservoirs (dark blue), DWDN (light blue; thin lines are distribution mains, and thick lines are transport mains), DHN (red), measurement locations (white stars), and areas for analysis (green): A and B for validation and calibration; A–E for sensitivity analysis (Appendix C.3).

The drinking water temperature was measured, with a resolution of ±0.05 °C, by Vitens employees at 35 locations on hydrants (see Figure 3) at two moments of the day

(one between 8:00 and 12:30 and one between 12:45 and 16:30), leading to a total of 70 data points. During the tests, the hydrants were opened with a low flow. Two areas (areas A and B; see Figure 3) were selected for the temperature measurements. According to Figure 2, these times should show a distinction in drinking water temperature changes for 110 mm pipes. The two areas have a similar year of installation and thus a similar design philosophy (with similar pipe diameters, materials, and network layout) and a similar number of residents (ca. 10,000 and 7000, respectively). They have a comparable residence time from the sources. The two areas likely differ in soil temperatures (see Table A8). The pipes in areas A and B have different installation depths and soil types. Also, in area A, a DHN is installed, potentially influencing part of the DWDN. In area B, there is no DHN.

The drinking water temperatures are expected to increase from the reservoirs during distribution as, in August, the soil temperatures are higher than the source water temperatures. A variation in temperature rise is expected due to differences in residence time and local soil temperature. Regarding the relevant pipe diameters, a residence time of a maximum of 15 h in the distribution areas (i.e., excluding the transport mains) is sufficient to capture the influence of the residence time (the red and yellow lines in Figure 2). The hydraulic model of the area (provided by Vitens) shows a residence time between 5 to 24 h for the whole network and a maximum of ca. 15 h in areas A and B (Table A9).

Five groups of pipes are distinguished: transport mains with and without DHN crossings, distribution mains in the older parts of the network with and without DHN crossings, and distribution mains in the newer parts of the network (only without DHN crossings). For these subgroups, a specific value of $T_{boundary}$ was determined with the STM for 31 August 2020 (see Table A8). In this case, study $T_{boundary}$ for stagnant water was used, based on the STM and not STM+. The reasons are (a) there are many uncertainties in the (STM) model parameters, e.g., soil type (λ_{soil}), which means that it was not possible to reliably model this case study site in STM+; (b) the difference between $T_{water,0}$ and the estimated $T_{boundary}$ is relatively large compared to the difference between $T_{boundary}$ in the active and passive mode, and the added value of modeling this case study with the STM+ seemed limited.

To simulate the drinking water temperature of Almere, the WTM+ (Equations (1) and (2)) was integrated into an Epanet-MSX model [20]; the parameters are given in Table A8. The results are temperatures at each time step and each node. For comparison with the measurements, the results at the nodes closest to the hydrant locations around the measurement time were taken from the model.

A sensitivity analysis for the WTM+ in a DWDN was performed on the case study (see Appendix C.3). It shows that the model is most sensitive to $T_{boundary}$ and TSoI. The larger the area where the (local) $T_{boundary}$ is imposed, the larger the number of customer nodes that are affected. For the WTM+ in a DWDN, λ_{soil} is not a very important parameter to estimate accurately, with the note that $T_{boundary}$, as estimated with the STM, is quite sensitive to λ_{soil}. The sensitivity to TSoI depends on the location in the network because of the residence time.

For model validation, the base case of Table 1 was used, for which the parameter values in Equation (2) are the best guesses from a priori knowledge of the area (see Appendix C.1). Because the sensitivity analysis shows that the WTM+ is very sensitive for TSoI and $T_{boundary}$, extra cases were introduced to calibrate the values for case study 2. Next, an optimization case was introduced, where the TSoI and $T_{boundary}$ were changed to find the best match to the measurements (minimum RMSE, maximum R^2). The optimal case is the best fit from the extra cases.

Table 1. The settings for the scenarios used for validation and calibration. Blanks are equal to the base case. Other parameter values are reported in Table A8. * The $T_{boundary}$ in the optimal and extra cases is applied with Equation (A11).

| Scenario	TSoI	T_{DM} °C	T_{DM_DHN} °C	T_{DM_NE} °C	T_{TM} °C	T_{TM_DHN} °C
Base case	1	18.7	19.5	20.5	18.0	20.1
Optimal case	2	20.1 *		20.1 *		
Extra cases	0.1–10	18.0–21.0 *		19.0–22.0 *		

3. Results

3.1. Case Study 1—Single Pipe

Figure 4 shows the measured and modeled temperatures. It shows that the incoming water temperature and soil temperatures were not constant over time.
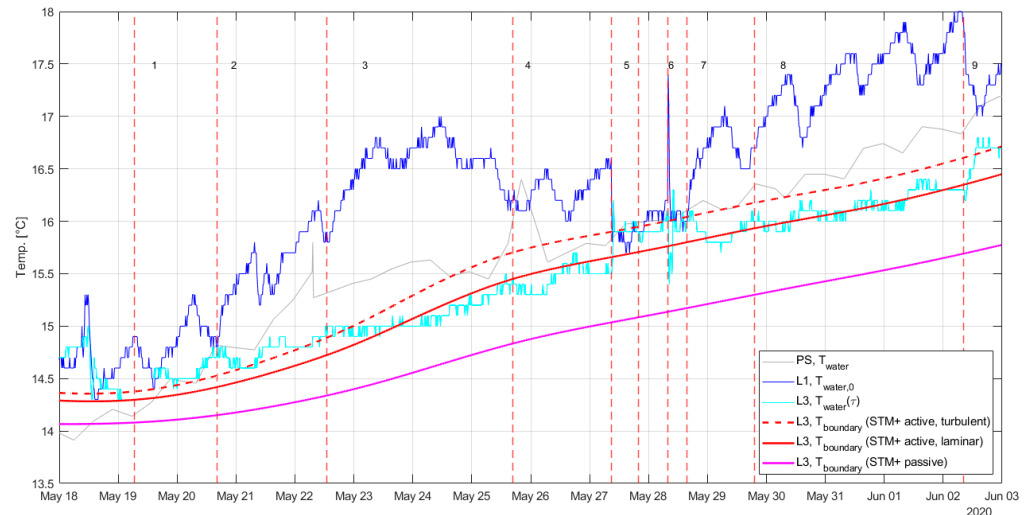
Figure 4. The measured drinking water temperatures and modeled soil temperatures for case study 1. The vertical dashed lines and numbers are the starting times of the 9 tests (see Table A1).

Figure 5 shows ΔTN versus the residence time with the measurement in boxplots and theoretical lines for various values of TSoI. The measurements at 1 and 2 h residence times were mostly discarded because of large measurement uncertainties. After filtering, there are no data points left with negative values, but there are still a few data points larger than 1. These are mainly found in test 4 (with a 12 h residence time).
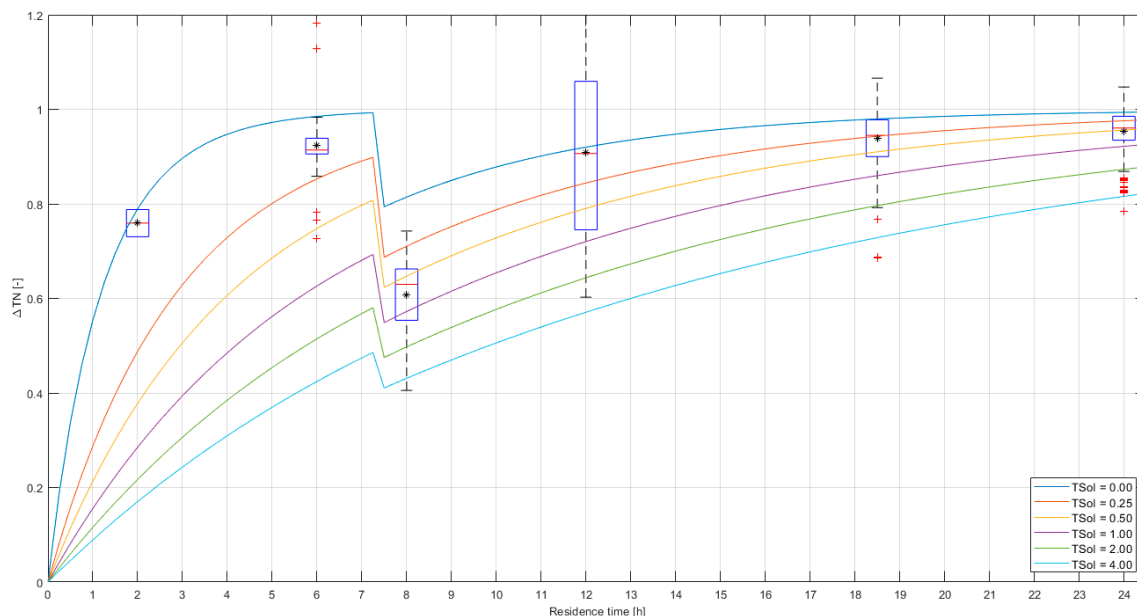
Figure 5. ΔTN versus residence time, with $T_{boundary}$ from STM+ active mode. Measured data are in boxplots, where the box represents the data between the 25th and 75th percentiles, the central red lines indicate the median, and the black star indicates the average. The whiskers extend to the most extreme data points not considered outliers, and the outliers are plotted as red plus symbols. The curves represent Equation (4), with different values for the TSoI. The threshold for turbulent flows is determined at $Re = 5000$. Data points (22) with $\Delta TN < 0$ are discarded. Data points (93) with $E \geq 0.5$ are discarded.

The theoretical lines depend on the Nusselt number, with a low *Nu* in the laminar flow regime and a high *Nu* in the turbulent flow regime. Typically, the literature suggests laminar flows at $Re < 2100$–2300, but turbulent flows can start anywhere at $Re > 3500$–10,000 [21]. Figure 4 shows that, at the start of tests 5, 6, and 9, the incoming water temperature changes very quickly, about 0.5 °C in the first few hours; this is not the case for the other tests. This may suggest that, for the high-flow tests, there is turbulent flow in the pipe upstream of L1 and therefore (the same pipe diameter, but slightly different flows) probably also between L1 and L3. For residence times of 8 h and more, we may assume laminar flows. In this case study, a residence time of 7 h means $Re \approx 5000$.

Figure 5 shows that the variability is large compared to the average values. It can be roughly estimated that the data correspond with values of TSoI between 0.0 (blue line) and 1.0 (purple line). As the variability of the data covers multiple theoretical lines, it is impossible to determine with enough certainty the correct value of TSoI.

Using Equations (1) and (2), the TSoI was calculated for each data point throughout each test. Figure 6 shows that the value for TSoI sometimes changes gradually over time, and sometimes the change is more abrupt. The spikes in the changes are explained by the inaccuracies of the measurements. To illustrate this, we examined test 3. Figure 4 (or more clearly in Figure A3) shows that $T_{water,0}$ increases gradually from 15.8 to 17 °C, although, due to the 0.1 °C accuracy, it does not look very gradual. The same can be said for T_{water} (*t*) increasing from 15 to 15.5 °C. $T_{boundary}$ increases from 14.8 to 15.3 °C. The difference between T_{water} (*t*) and $T_{boundary}$ is typically less than 0.1 °C, or, given the measurement inaccuracies, the difference is between 0 and 0.2 °C. In Equation (4), this means that the denominator and the numerator are the same plus or minus 0.2 °C, or $\Delta TN \approx 1$. At first, T_{water} (*t*) − $T_{water,0}$ = 1.0 °C, or ΔTN = 0.8–1.2, and, after 24 h, T_{water} (*t*) − $T_{water,0}$ = 1.5 °C or ΔTN = 0.9–1.1. This explains the relatively large spikes in TSoI, with a decrease over time. The values smaller than 0 have no physical meaning and can also be explained by the uncertainty in the parameters of Equation (4). Figure 6 thus clearly illustrates the effect of measurement uncertainty. As $(T_{water,0} - T_{boundary}) \approx 0.6$ to 1.6 °C during the test period (Figure A3), it is impossible to have highly accurate results where $(T_{water} - T_{boundary}) > 0.2$ °C. In the calculations, it follows that, if $D_3 = D_2$ (TSoI = 0), $(T_{water} - T_{boundary})$ would be smaller than 0.1 °C for all tests, except for test 1 (0.13 °C). Even if $D_3 >> D_2$ (e.g., TSoI = 20), $(T_{water} - T_{boundary}) > 0.1$ °C only for tests 1, 2, 4, 7, and 9. It is important to note that $(T_{water,0} - T_{water}) > 0.5$ °C for all tests. This means that, for TSoI, we should consider the average of the calculated values; the instantaneous values are not reliable enough.
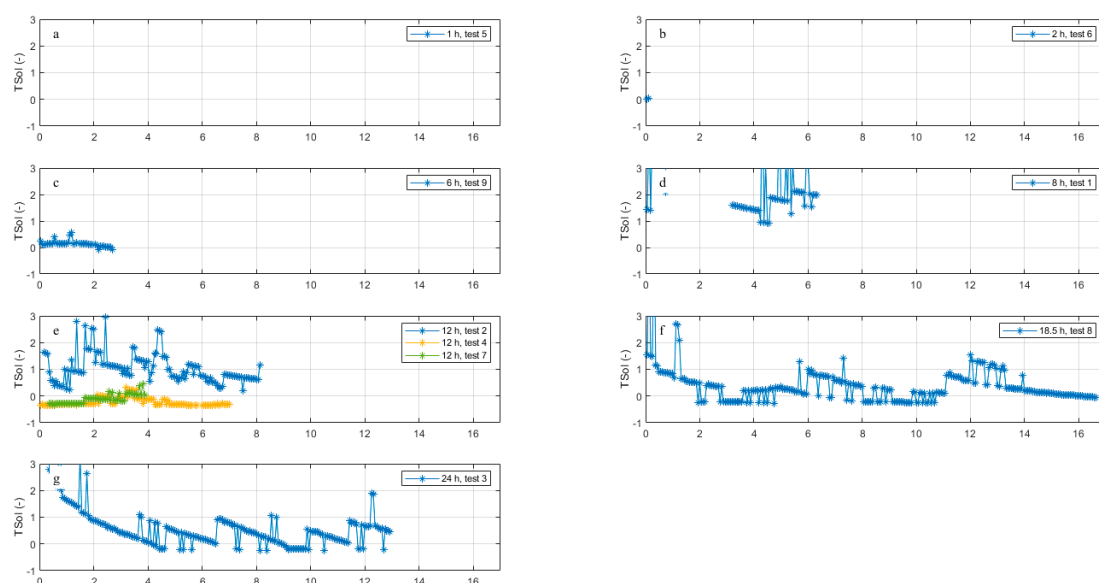

Figure 6. The calculated TSoI for all data points against time (h) on the horizontal axis since the start of the test. Tests with residence time of (**a**) 1 h (test 5); (**b**) 2 h (test 6); (**c**) 6 h (test 9); (**d**) 8 h (test 1); (**e**) 12 h (test 2, 4, 7); (**f**) 18.5 h (test 8); (**g**) 24 h (test 3).

Figure 6 also shows a decrease in TSoI over time. The tests at an 18.5 and 24 h residence time have a TSoI of 1 to 3 at the start of the test and a TSoI of 0 to 1 at the end. The test at 8 h (test 1) and the first test at 12 h (test 2), i.e., the first two tests, show higher values (TSoI = 1–2) than the later tests (tests 4, 7, and 9 with TSoI ≈ 0).

The same data processing was performed with $T_{boundary}$ from the STM+ passive mode calculations. The results are shown in Figure A5. In these calculations, fewer data points were discarded because $(T_{boundary} - T_{water,0})$ was larger. However, the uncertainty due to $(T_{water} - T_{water,0})$ is still significant. This exercise leads to estimates of TSoI = 5–10, where under none of the imposed residence times does T_{water} (almost) equal $T_{boundary}$. The results from the passive mode are located in Appendix B.4, because, in case study 2, TSoI values are much closer to those from the results of the active mode.

3.2. Case Study 2—DWDN

Figure 7a shows the base case with TSoI = 1, the simulated drinking water temperature, at the model nodes, as well as the time corresponding to the measurements versus the measured drinking water temperature. As the morning and afternoon measurements showed a maximum variation of ca 1 °C, all data are considered as a single dataset [22]. Areas A and B are distinguished as they have different values for $T_{boundary}$. There are two locations (H1330 and H1357 in area B) where the measured drinking water temperature is ca. 3.5 °C lower than the model results and one location (H5870 in area A) where the measured drinking water temperature is ca. 2.5 °C higher than the model results. The deviations were found for both the morning and afternoon measurements, so a measurement error is not a likely cause. There are no known local hot or cold spots that may cause the deviations. It may be that one or more valves in the DWDN are different from what the model assumes, leading to longer or shorter residence times (and thus higher or lower temperatures) than what the model would calculate. This would mean that, for these locations, the hydraulic model does not calculate the correct residence time, and these locations would not be suitable for validating the WTM+. The validation results are shown for all 70 measurements and the subset of 64 measurements where the measurements of these three locations are excluded (referred to as outliers). It is important to note that the optimal case shows the same data points as potential outliers.
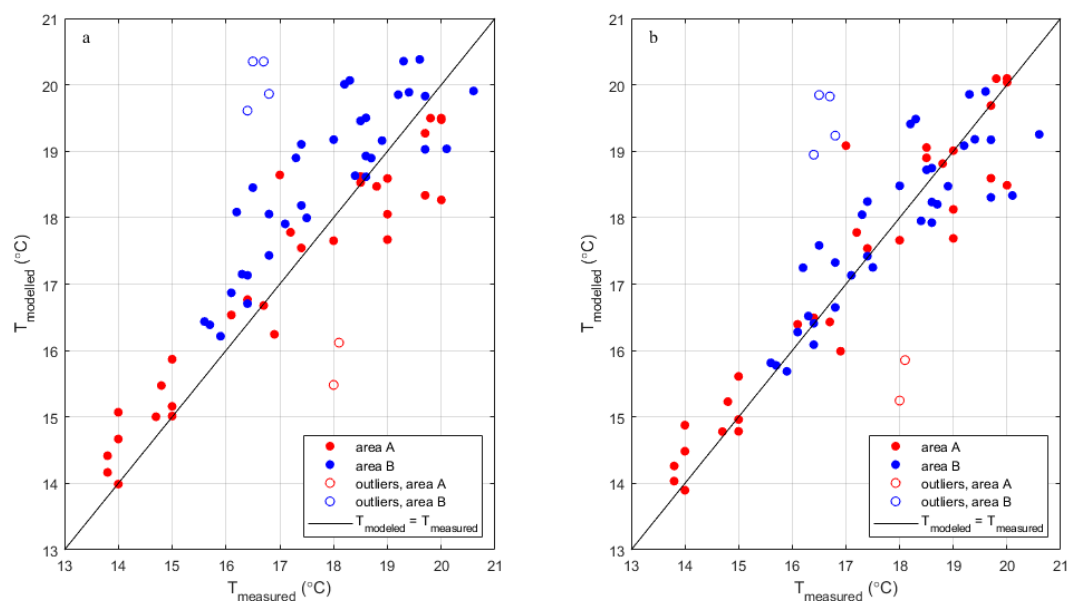
Figure 7. The validation of WTM+. The model results are compared to field measurements, and open circles indicate outliers in area A (red, below the line) and area B (blue, above the line) for (**a**) the base case, TSoI = 1, and (**b**) the optimal case with adjusted $T^*_{boundary}$ = 20.1 °C and TSoI = 2.

The maximum drinking water temperature measured in area A is 20 ± 0.05 °C, and, in area B, it is 20.6 ± 0.05 °C. The maximum drinking water temperature simulated for the measurement locations in area A is 19.5 °C (corresponding to T_{DM_DHN}), and, in area B, it is 20.5 °C (corresponding to T_{DM_NE}). The uncertainty in the model is unknown. For the data in Figure 7a, the model fits the measurements better in area A than in area B with respect to the root mean square error (RMSE) and the Pearson correlation coefficient R^2 (Table A11).

A change in TSoI has the largest effect on the temperatures at lower residence times, and a change in $T_{boundary}$ has the largest effect on the temperatures at higher residence times. Changing both parameters simultaneously (the extra cases) may lead to a smaller RMSE or larger R^2. Table A11 shows that the RMSE decreases from 1.5 °C (without outliers) to 0.76 °C with an increase in the TSoI from 0.05 to 2 and then increases again for TSoI > 2. At the same time, the R^2 increases from <0 (without outliers) to 0.80 and then decreases.

The result with the lowest RMSE and highest R^2 is found for $T_{boundary} = 20.1$ °C and TSoI = 2 (Table A11, both areas together; this is referred to as the optimal case). Figure 7b shows this graphically. The fit for area A is better than for area B. For areas A and B, the optimum is not found at the same $T_{boundary}$—which can be expected as the pipe installation depth and soil types differ in the two areas—nor at the same TSoI, which has not been explained. In the validation for case study 2, the a priori estimates of the soil temperatures (base case) and TSoI = 1–2 lead to the best fit. In the calibration for case study 2 with the a posteriori estimates of the soil temperatures (extra case), TsoI = 2–3 leads to the best fit.

4. Discussion

4.1. Reflection on the Model Approach

In general, the two case studies show a reasonable match between modeled and measured temperatures, as shown in Figures 5 and 7. In both cases, however, the spread in the measured temperatures also reveals plenty of case-by-case deviations. At least in part, these deviations are caused by the approximations inherent to the modeling approach.

The most crucial approximations involve introducing a two-step approach through the coupled STM and WTM models. In the first step—the STM+—a characteristic, steady-state interaction between pipe and environment is determined based on a simulation of a given, two-dimensional cross-section of the system perpendicular to the water flow. This characteristic situation is then transferred to the second step—the WTM+—to evaluate the temperature of the water when it travels through this characteristic situation for a prolonged duration. This approach keeps the model practically manageable, unlike a fully detailed, dynamic model in three spatial dimensions of a complete distribution network and its environment. However, the approach also leads to the simplification of several aspects.

The first aspect is that, in the STM+, general assumptions about the soil, built environment, local weather, etc., must be made, which are then taken to represent large parts of the network. In other words, the WTM+ assumes a limited number of values of $T_{boundary}$ over space and time. Blokker and Pieterse-Quirijns [4] established that the soil temperature 1 m below ground level varies no more than 1 °C per day. As typical drinking water residence times (hours) are in the same order of magnitude, it seems a reasonable approximation to ignore temporal variations in $T_{boundary}$. The spatial variation most likely should not be ignored.

A second aspect concerns the assumption that $T_{boundary}$ in Equation (1) is not influenced by the drinking water temperature. Figure 1b illustrates that we assume that, over (the residence) time (over the length of the pipe), the tangent to the temperature gradients in the soil is such that there is a constant $T_{boundary}$ at a specific value of D_3. A third aspect, following the second, concerns the assumption that the temperature gradients in the soil around the drinking water pipes are well-developed, semi-steady profiles. This assumption is unlikely to be true as the drinking water temperature and flow rate in a real DWDN are never constant. The temperature of the drinking water source may change, and the flow velocity of the water changes with daily demand patterns. Both these aspects are related to how the STM+ and WTM+ are coupled. As case study 1 indicates that TSoI may not be

constant (Figure 6), this assumption of coupling the STM+ and WTM+ may not be valid. An extensive three-dimensional modeling approach is required to validate this assumption or determine a better way of coupling.

4.2. Estimation of TSoI

The WTM+ does not describe the real heat exchange through the soil around the pipe. Therefore, the thickness of the soil layer is not a real physical entity but serves the purpose of mimicking a decrease in the heat exchange rate. This also means that the fact that $T_{boundary}$ from the STM+ is more or less constant over TSoI = 0.2 to 1 (not tested for larger values) does not help to determine the value of D_3. It is expected that a temperature change in the drinking water will mean that, after a few hours, only a small layer of the soil around the drinking water pipe will be affected. The STM+ can be used to determine the value of this penetration depth. However, the meaning of this for the value of D_3 is unclear. This means that the value of D_3 (or of the TSoI) is not known a priori. In this study, we tried to deduce the value from measurements. An alternative would be to deduce it from an integrated model.

The values for D_3 that we found in the literature can be converted into equivalent values of TSoI with the help of Equation (1). Hubeck-Graudal et al. [8] used the total heat transmission coefficient between soil and drinking water. They included the conductive heat resistance of the soil plus a correction factor for the convective resistance at the soil surface. We found $D_3 \approx 4(H + 0.1)$, with H equal to the burial depth. For case study 1, with $D_1 = 160$ mm, $D_2 = 150$ mm and $H = 1$ m, TSoI = $(4(H + 0.1) - D_2)/2D_1 = 13.9$. De Pasquale et al. [7] used $D_3 = D_2 + 2l = D_2 + 2\sqrt{\frac{\alpha_{soil}}{\omega}} = D_2 + 2\sqrt{\frac{8.0E-7}{1.992E-7}}$, so $TSoI = \frac{\sqrt{\frac{\alpha_{soil}}{\omega}}}{D_1} = 13.2$, with ω being 2π divided by the number of seconds in one year. Hypolite et al. [10] developed the Barletta method, which uses the soil temperature at the pipe burial depth as a boundary condition and a shape factor to define D_3. If $2H >> D_2$, then $D_3 \approx 4H$, and TSoI = $(4H - D_2)/2D_1 = 12.6$. Díaz et al. [9] assumed that $D_3 = H$, and thus TSoI = $(H - D_2)/2D_1 = 2.8$. For case study 2, for the most dominant diameters, $D_1 = 110$ mm, $D_2 = 100$ mm, and $H = 1$ m, the TSoI values are 21.5, 20.0, 19.5, and 4.5, respectively. The values of the first three [7,8,10] are comparable, on average, to TSoI = 13.2 and 20.3 for case studies 1 and 2, respectively; they seem to largely overestimate our results of TSoI = 0.0–3.0. The values found by Díaz et al. [9]—2.8 and 4.5—are closer to what we found. It is remarkable that the approaches from these authors all assume a thermal sphere of influence independent of the pipe diameter.

Case study 1 (Figure 6) shows that the TSoI was not constant throughout the test. In the first few hours after a sudden change in residence time, TSoI equals 2 to 3 and then decreases to 0 to 1. For turbulent flows, the low TSoI value is reached faster than for laminar flows. Case study 2 (Table A11) shows that the optimal TSoI differs for areas A and B, with TSoI = 1 to 2 and 2 to 3, respectively. In a real network, the flows change constantly, and the conditions are more equal to the first phase of the tests in case study 1. This means that a TSoI = 2 is recommended for laminar flows. For turbulent flows, a smaller TSoI (0 to 1) seems more appropriate.

For a TSoI > 0, the heat transfer rate k for the WTM+ is smaller than for the WTM ($D_3 = 0$). For a Ø110 PVC pipe, a TSoI = 2 means that, for high flow rates ($Nu = 100$), k is reduced by 36%, and by 60% for low flow rates ($Nu = 3.66$); for a Ø160 PVC pipe, the values are 27% and 57%, respectively. This means that a considerably longer contact time is needed before the drinking water will have reached the soil temperature than was assumed by Blokker and Pieterse-Quirijns [4]. For a distribution network of Ø110 PVC pipes, a residence time of 12 h is needed instead of 4 h. It is important to note that, as, typically, residence times are longer, the conclusion by Blokker and Pieterse-Quirijns [4] still holds: most customers will experience drinking water temperatures equal to the soil temperature at a 1 m depth.

4.3. Recommendations for Validation Measurements

Extra measurements are recommended for model validation, especially to better understand the TSoI over time and if the TSoI is independent of the pipe diameter. This means that measurements over a range of pipe diameters, including one larger than 160 mm, are required.

We encountered various challenges in the validation process; the learning points are summarized into recommendations for measuring (Table 2). In both case studies, the many boundary conditions are continuously changing, are unknown, or are difficult to assess. The two case studies have different strengths and weaknesses [22]. In case study 1, many parameters were well known and approximately stable over the pipe length. However, the differences in the three temperature parameters were relatively small, which meant that the accuracy of the thermal sensor was not high enough. In case study 2, various parameters were not well known. Here, the differences between drinking water and soil temperature were large enough to hardly be affected by measurement uncertainties, and measurements were duplicated (morning and afternoon).

Table 2. An overview of case studies and recommendations for measurements.

	Case Study 1	Case Study 2	Recommendation for Measurements
Trajectory	Single pipe	DWDN	Single pipe, measured at 3 or more locations over pipe length
D_1 (mm)	152	101 (51% of length)	Range of diameters
Length (km)	0.9	Ca. 700	Result from Q and τ
τ (h)	1, 2, 8, 12, 18, 24	5–24	Use model to estimate the range of interest (depends on D_1) and measure at three or more τ, plus at very large τ
Q (m^3/h)	Controlled (1, 4 to 0.06)	Result of demands	Use flows both in laminar and turbulent regimes
Duration	2 weeks (2 h to 2 days per test)	1 day (morning, afternoon)	2–5 days per test
# data points	870 (41 to 266 per test)	72	>40 per test; duplicate each test
Water source	Surface water	Groundwater	Groundwater
Season	Spring	Summer	Summer, winter
Parameters that are known accurately	D_1, D_2, λ_{soil}, λ_{water}, λ_{pipe}, α_{water}, τ (Q, Re), $T_{boundary}$, T_{water}, $T_{water,0}$	D_1, D_2, λ_{water}, λ_{pipe} (but PVC was assumed for all pipes in the model) α_{water}, T_{water}, $T_{water,0}$	D_1, D_2, λ_{soil}, λ_{water}, λ_{pipe}, α_{water}, τ, Nu, $T_{boundary}$, T_{water}, $T_{water,0}$
Strength	Many parameters are known accurately. Parameters are constant over space	Absolute temperature differences are significant. Parameters are constant over time	Many parameters are known accurately. Absolute temperature differences are significant. Parameters are constant over space or time
Weakness	Absolute temperature differences are small. Flow is enforced, not natural, and there may not be a natural equilibrium Nusselt not known	Residence time and $T_{boundary}$ are not accurately known Nusselt is not known	

A single pipe stretch allows for the best estimate of all parameters. To measure temperature after a residence time under both turbulent and laminar flow regimes, sensors should

be placed at several locations along the pipe length. It is recommended to measure during summer (or winter) in a groundwater-fed system to ensure measurement uncertainties of T_{water} and $T_{water,0}$ that are small relative to the temperature differences.

It is important to note that $T_{boundary}$ is a model parameter from the STM+. By definition, $T_{boundary}$ can only be measured when the drinking water and soil temperature are in equilibrium. For the STM+ passive mode, $T_{boundary}$ can be validated in stagnant water by measuring the temperature of the drinking water. For the STM+ active mode, $T_{boundary}$ can be validated in flowing water by measuring the drinking water at a very high residence time (the value depends on pipe diameter). Be aware that, as the weather conditions are never constant, $T_{boundary}$ is, at best, a dynamic equilibrium.

4.4. Practical Application

The 25 °C norm for drinking water in the Netherlands is threatened by, e.g., the installation of a DHN parallel to the DWDN and climate change. Large-scale replacement programs for an aging DWDN and urban developments in greening urban areas allow for distinctive choices with respect to DWDN installation, e.g., enforcing a minimum distance between the DHN and DWDN or installing the DWDN under grass. As a DWDN typically can last for more than 100 years, the time to take measures to prevent high drinking water temperatures is in the coming years. The developed models allow us to quantify the effect of various scenarios and countermeasures. For example, the modeling approach supported determining the minimum distances between DHN and DWDN pipes. First, it became clear that, even without the DHN, the drinking water temperatures may sometimes exceed 25 °C. Therefore, the acceptance of a maximum of a 1 °C increase in the drinking water temperature due to the DHN was decided. It also became clear that, to ensure this maximum increase in the entire DWDN, the distances between the DHN and DWDN would have to be very large, leading to a situation where, in practice, the installation of a DHN could not occur. Instead, the maximum increase was imposed on 95% of the customer connections. Based on a large set of realistic scenarios (WTM+ on the Almere DWDN, with $T_{boundary}$ from the STM+ for various distances between the DWDN and DHN of various diameters and temperatures), the minimum distance was determined as 1.5 m (wall to wall), with the option of 1.0 m for a maximum of 25% of the DWDN length or 0.5 m for a maximum of 5% of the DWDN length [23].

5. Conclusions

In this study, we enhanced the water temperature model from Blokker and Pieterse-Quirijns [4] into a WTM+ that includes a thermal sphere of influence (TSoI), which accounts for the soil not having an infinite heat capacity. The soil temperatures are affected by climate factors, soil type, soil cover, and (subsurface) anthropogenic heat sources, and the boundary conditions for the WTM+ are modeled with the STM+. We applied the WTM+ on a single pipe and a DWDN over a range of relevant residence times. We used measurements in these case studies to show the validity of the WTM+ and its coupling to the STM+ and determine the value of the TSoI.

Case study 1 showed that using the WTM+ with $T_{boundary}$ from the STM+ and a TSoI of ca. 1 improves the old WTM. Calibration was a challenge because some boundary conditions and model parameters could not be accurately determined and had to be estimated. The Reynolds number, above which conductive and convective heat exchange between the pipe wall and the drinking water were found, was estimated at 5000.

Case study 2 allowed for a validation in a DWDN. Given all uncertainties, an RMSE of under 1.0 °C and $R^2 > 0.7$ is quite good, and using a TSoI of 2 improved the results.

In the two case studies, applying the STM+ and WTM+ together can accurately describe the drinking water temperature change over time throughout a network.

Appendix A. Equations for Error Estimation

In this appendix, shorter symbols are used for T_{water} (=T_w), $T_{water,0}$ (=$T_{w,0}$), and $T_{boundary}$ (=T_b).

$$\Delta TN = \frac{T_{water} - T_{water,0}}{T_{boundary} - T_{water,0}} = \frac{T_w - T_{w,0}}{T_b - T_{w,0}} \tag{A1}$$

$$
\begin{aligned}
E_1 &= \frac{T_w + \varepsilon_w - T_{w,0} + \varepsilon_w}{T_b + \varepsilon_s - T_{w,0} + \varepsilon_w} - \frac{T_w - T_{w,0}}{T_b - T_{w,0}} \\
&= \frac{(T_w - T_{w,0} + 2\varepsilon_w)(T_b - T_{w,0}) - (T_w - T_{w,0})(T_b - T_{w,0} + (\varepsilon_w + \varepsilon_s))}{(T_b - T_{w,0})(T_b - T_{w,0} + (\varepsilon_w + \varepsilon_s))} \\
&= \frac{2\varepsilon_w(T_b - T_{w,0}) - (\varepsilon_w + \varepsilon_s)(T_w - T_{w,0})}{(T_b - T_{w,0})(T_b - T_{w,0} + (\varepsilon_w + \varepsilon_s))}
\end{aligned}
\tag{A2}
$$

$$
\begin{aligned}
E_2 &= \frac{T_w - T_{w,0}}{T_b - T_{w,0}} - \frac{T_w - \varepsilon_w - T_{w,0} - \varepsilon_w}{T_b - \varepsilon_s - T_{w,0} - \varepsilon_w} \\
&= \frac{-(T_w - T_{w,0} - 2\varepsilon_w)(T_b - T_{w,0}) + (T_w - T_{w,0})(T_b - T_{w,0} - (\varepsilon_w + \varepsilon_s))}{(T_b - T_{w,0})(T_b - T_{w,0} - (\varepsilon_w + \varepsilon_s))} \\
&= \frac{2\varepsilon_w(T_b - T_{w,0}) - (\varepsilon_w + \varepsilon_s)(T_w - T_{w,0})}{(T_b - T_{w,0})(T_b - T_{w,0} - (\varepsilon_w + \varepsilon_s))}
\end{aligned}
\tag{A3}
$$

$$\overline{E} = \frac{E_1 + E_2}{2} \tag{A4}$$

$$\overline{E} = \frac{2\varepsilon_w(T_b - T_{w,0}) - (\varepsilon_w + \varepsilon_s)(T_w - T_{w,0})}{2(T_b - T_{w,0})} \times \left(\frac{1}{T_b - T_{w,0} + (\varepsilon_w + \varepsilon_s)} + \frac{1}{T_b - T_{w,0} - (\varepsilon_w + \varepsilon_s)} \right) \tag{A5}$$

$$
\begin{aligned}
\overline{E} &= \frac{2\varepsilon_w(T_b - T_{w,0}) - (\varepsilon_w + \varepsilon_s)(T_w - T_{w,0})}{2(T_b - T_{w,0})(T_b - T_{w,0} + (\varepsilon_w + \varepsilon_s))(T_b - T_{w,0} - (\varepsilon_w + \varepsilon_s))} \\
&\times (T_b - T_{w,0} - (\varepsilon_w + \varepsilon_s) + T_b - T_{w,0} + (\varepsilon_w + \varepsilon_s))
\end{aligned}
\tag{A6}
$$

$$\overline{E} = \frac{2\varepsilon_w(T_b - T_{w,0}) - (\varepsilon_w + \varepsilon_s)(T_w - T_{w,0})}{2(T_b - T_{w,0})\left((T_b - T_{w,0})^2 - (\varepsilon_w + \varepsilon_s)^2 \right)} \times 2(T_b - T_{w,0}) \tag{A7}$$

$$\overline{E} = \frac{2\varepsilon_w(T_b - T_{w,0}) - (\varepsilon_w + \varepsilon_s)(T_w - T_{w,0})}{(T_b - T_{w,0})^2 - (\varepsilon_w + \varepsilon_s)^2} \tag{A8}$$

If ε_s is small:

$$\overline{E} = \frac{\varepsilon_w(2T_b - T_{w,0} - T_w)}{(T_b - T_{w,0})^2 - \varepsilon_w^2} \tag{A9}$$

If $\varepsilon_s = -\varepsilon_w$:

$$\overline{E} = \frac{2\varepsilon_w}{(T_b - T_{w,0})^2} \tag{A10}$$

Appendix B. Case Study 1

Appendix B.1. Additional Information on Case Study 1

Case study 1 is a single pipe: a Ø160 mm PVC pipe (D_1 = 152 mm, D_2 = 160 mm) in Rotterdam with a length of 925 m. This pipe is fed from a surface water PS (pumping station) through a stretch "S1" of 1650 m (D_1 = 1569 mm), "S2" of 1350 m (D_1 = 1369 mm), and "S3"of 570 m (D_1 = 150.6 mm); see Figure A1. The water in the measured pipe flows from location L1 to location L2 (stretch "S4"—415 m) to location L3 (stretch "S5" 510 m). The flow at L3 was controlled with a hydrant. During a two-week measurement period (19 May 2020–3 June 2020), the flow rate was regulated in order to obtain measurements for residence times of the water in the pipe from 1 to 24 h.
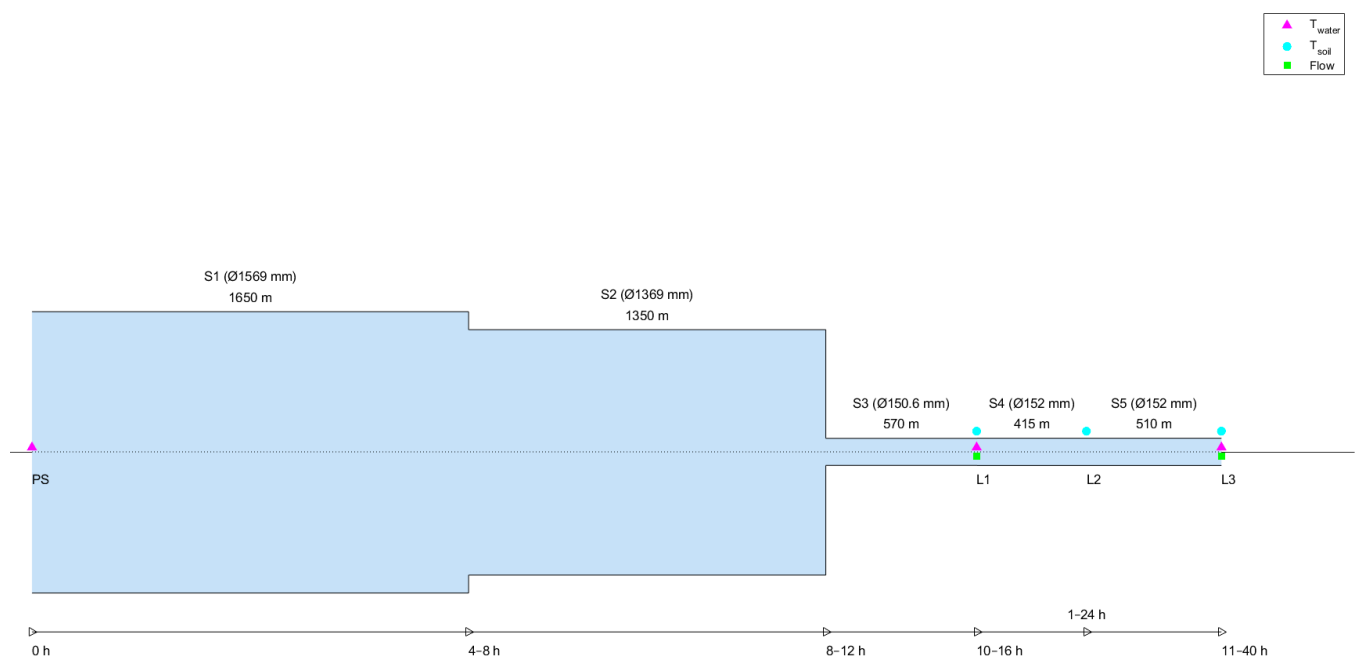
Figure A1. The measurement locations of case study 1. In green, flow meter locations, in magenta and cyan, drinking water temperature and soil temperature measurement locations. Stretch names with length and diameter are indicated above, and residence times are indicated below. PS is pumping station, L1, L2, and L3 are measurement locations.

The following were measured, with a logging frequency of once per 15 min:

- T_{water} was measured at the PS and at L1 and L3 (Figure 4). We may assume that T_{water} at the start of S3 is equal to T_{water} from the PS as S1 and S2 have large diameters and short residence times. However, T_{water} at the end of S3 (location L1) is not equal to T_{water} from the PS (Figure 4).
- T_{soil} (temperature of the soil) was measured at L1, L2, and L3, at various distances from the pipe.
- The flow was measured at L1 and L3. During the measurements, there was limited demand from customers along the pipe, as there is only one residential customer, and some sports facilities that were closed during the COVID-19 pandemic. The demand at the customer location was measured, and it had a negligible effect on the flow at L1. The residence time between L1 and L3 was calculated from the pipe length, pipe diameter, and flow at L3.
- Note that the flow through stretches S1, S2, and S3 are not measured.

During the test, changing the settings took 15–30 min; this explains the differences between the end time and starting times in Table A1. Test 1 started on 18 May 2020, but some measurements were lost. Therefore, we used data from 19 May onwards. Test 6 was started 15 min after test 5 ended. However, a passerby closed the hydrant. The next morning, during the check, test 6 was started again. The measurements at L1 were stopped at 3 June 0:45. Table A1 shows the calculated residence time, Reynolds number, and Nusselt number for the case study.

Table A1. Test information: start and end time (2020), flow rates, residence time, and calculated Reynolds and Nusselt numbers (at 16 °C, average of the measured incoming water), with $Nu = 3.66$ for $Re < 5000$; $Nu = 0.027\ Re^{0.8}\ Pr^{0.33}$ for $Re > 5000$.

ID	Start Time	End Time	Flow Rate [m³/h]	Residence Time [h]	Re [10^3]	Nu [-]
1	19 May 6:30 (18 May 12:00)	20 May 16:00	2.1	8.0	4.4	3.66
2	20 May 16:15	22 May 12:30	1.4	12.0	2.9	3.66
3	22 May 13:00	25 May 16:30	0.7	24.0	1.5	3.66
4	25 May 16:45	27 May 08:30	1.4	12.0	2.9	3.66
5	27 May 09:15	27 May 20:00	16.7	1.0	35.0	221.49
6	28 May 08:00	28 May 15:00	8.5	2.0	17.8	129.04
7	28 May 15:30	29 May 18:45	1.4	12.0	2.9	3.66
8	29 May 19:00	2 June 07:45	0.9	18.6	1.9	3.66
9	2 June 08:15	3 June 10:00	2.8	6.0	5.9	53.08

After the nine tests were conducted, the sensors were calibrated in the lab. The calibration consisted of two days measuring the same water at a temperature between 16.5 and 18.5 °C. Figure A2 shows the error between the two sensors measuring T_{water} at L1 and L2 (error $T_{water} - T_{water,0}$) and between the sensors measuring T_{water} at L1 and T_{soil} (error $T_{water} - T_{soil}$). It can be seen that T_{water} at L1 was usually lower than what the soil temperature sensors and the sensor T_{water} at L2 measured.
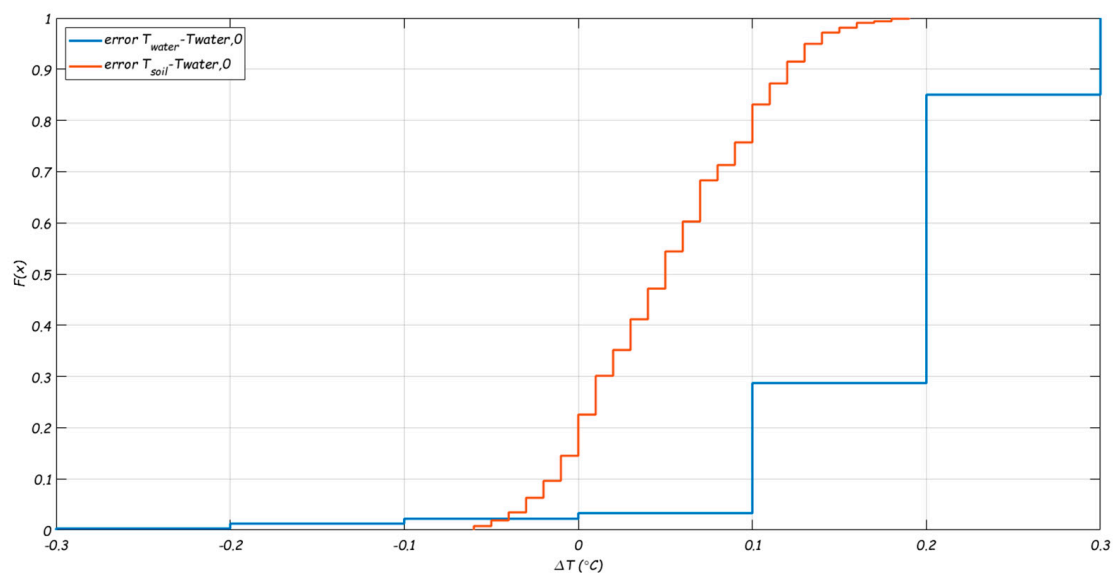
Figure A2. Cumulative frequency distribution of the difference between temperature sensors during calibration.

The values that were used in the WTM+ for case study 1 are listed in Table A2.

Table A2. Parameters values of Equation (2) and (4) for case study 1. Constants for water are used ($\rho_{water} = 1000 \text{ kgm}^{-3}$, $C_{p,water} = 4.19 \text{ Jkg}^{-1}\text{K}^{-1}$, $\lambda_{water} = 0.57 \text{ Wm}^{-1}\text{K}^{-1}$, $\alpha_{water} = 0.14 \text{ m}^2\text{s}^{-1}$).

Parameter	Unit	Value	Uncertainty	Reference
D_1	mm	152	-	Information from water utility Evides
D_2	mm	160	-	
Nu	-	Table A1	Unclear beforehand where transition between turbulent and laminar flow is found	For turbulent flows: $Nu = 0.027\ Re^{0.8}\ Pr^{0.33}$ For laminar flows: $Nu = 3.66$ [4]
λ_{pipe}	$\text{Wm}^{-1}\text{K}^{-1}$	0.16	-	PVC [4]
D_3	mm	$D_2 + \text{TSoI} \times D_1$		To be determined
λ_{soil}	$\text{Wm}^{-1}\text{K}^{-1}$	1.6	$\pm 0.3\ °C$	Measured [17]
$T_{water,0}$	°C		$\pm 0.1\ °C$	Measured (L1)
T_{water}	°C	Time series, Figure 4.	$\pm 0.1\ °C$	Measured (L3)
$T_{boundary}$	°C		$\pm 0.1\ °C$	For flowing water, from STM+

Appendix B.2. Measurement Data Processing

To validate the WMT+ with these measurements, we need to consider that none of the parameters in Equation (4) are constant over time. It is required to perform some data processing in order to match measurements at the beginning and end of the pipe and to ensure that the data can be compared over time.

The normalized temperature difference ΔTN (Equation (4)) is calculated for every (15 min) data point (Table A3). The parameters are determined as follows:

- $\tau(t)$: the residence time follows from the measured flows.
- $T_{water,0}(t)$: drinking water temperature measured at location L1.
- $T_{water}(\tau, t)$: drinking water temperature measured at location L3, corrected for residence time τ ($T_{water}(\tau, t) = T_{water}(t + \tau)$). For example, for test 4, $Q = 1.4 \text{ m}^3/\text{h}$ and thus $\tau = 5$ (L1 to L2) + 7 h (L2 to L3). Therefore, at L3, $T_{water}(\tau, t) = T_{water}(t + 12)$, where the data during the transition time of 12 h are discarded. Table A3 shows the residence times and the amount of data points left for the analysis after discarding the transition period (see also Figure A3).
- $T_{boundary}(t)$: $T_{boundary}$ was estimated with the STM+ results for L3. We thus assume that the same boundary condition is valid for the entire pipe length between L1 and L3. For the tests, we assume that, during the residence time, the $T_{boundary}$ that is experienced by the flowing water is the average of the modeled soil temperature during this residence time: $T_{boundary}(t) = mean\left(T_{boundary,\ STM+}(t : t + \tau)\right)$ (see also Figure A3). Note that $T_{boundary}$ for flowing water was used for turbulent and laminar flows. In Figure A5, the test results with $T_{boundary}$ for stagnant water are shown.

With respect to the uncertainties (ε_w in T_{water}, ε_s in $T_{boundary}$), the following are noted:

- $\tau(t)$: the accuracy can be estimated as $\Delta\tau/\tau \approx \Delta Q/Q$. The accuracy of the flow meter is 0.004 m³/h (1 liter with a log frequency of 15 min). During the test phases, the flow is kept more or less constant, and the accuracy plus variability lead to a ΔQ equal to 0.012 m³/h. For the flow rates of Table A1, this results in less than 1 min for the short residence times of test 5 and 6 ($\tau = 1$ and 2 h, respectively) and almost 30 min for the longest residence time of test 3 ($\tau = 24$ h). This means an uncertainty in the residence time of less than 2%, and therefore, it is neglected.
- ΔTN: the accuracy is related to the accuracy of drinking water temperature measurements. The accuracy in $T_{water,\ 0}$ and $T_{water}(t)$ is $\pm 0.1\ °C$. The calibration that was carried out after the measurement period showed an average error between the two sensors at L1 and L3 (i.e., $T_{water,\ 0}$ and $T_{water}(t)$) of 0.2 °C ($2 \times \varepsilon_w = 0.2\ °C$, Figure A2). The uncertainty for the modeled $T_{boundary}$ is estimated as 0.1 °C [17]. When these errors have the opposite sign, the largest error will occur. With $\varepsilon_w = -\varepsilon_s = 0.1\ °C$, the uncer-

tainty in ΔTN is determined as (see Appendix A) $\overline{E} = \dfrac{2\varepsilon_w}{\left(T_{boundary}-T_{water,0}\right)^2}$. This means that, when $(T_{boundary} - T_{water,\,0})$ is small, the uncertainty in ΔTN is large. This uncertainty is not negligible. Figure A4 shows 985 data points with their corresponding normalized temperature difference (ΔTN and uncertainty bars).
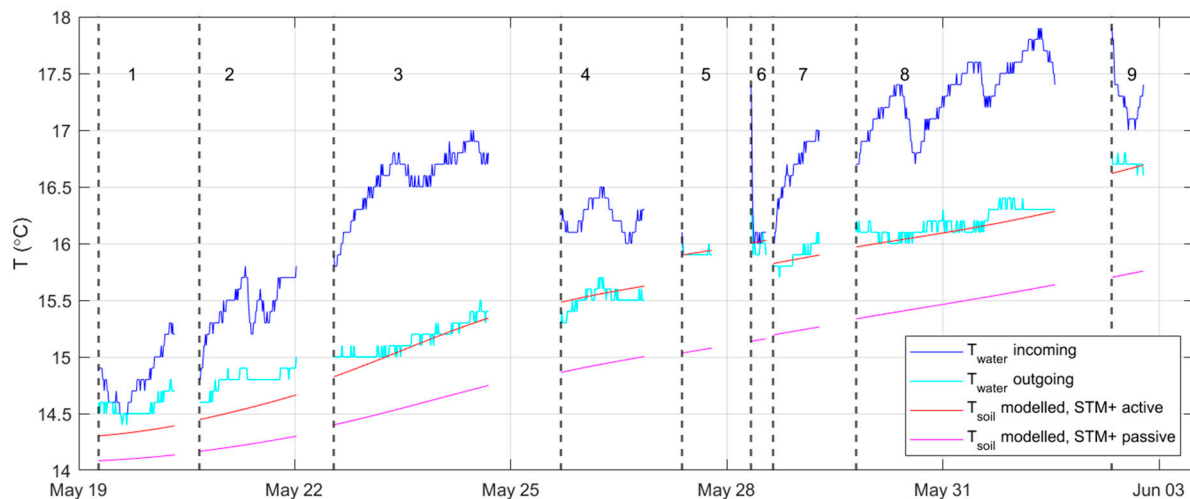
Figure A3. The parameter values for Equation (4) after adjustment for residence time and selection of laminar and turbulent flows ($Re > 5000$) in the active mode and the passive mode (where no distinction in flow regime is made). The vertical dashed lines and numbers are the starting times of the 9 tests (see Table A1).

The vast majority of the data points showed a decrease in the measured drinking water temperature ($T_{water}(t) < T_{water,\,0}$). For 22 of 985 data points (indicated with black error bars in Figure A4), the situation was reversed, with a decrease of 0.1 °C (15 data points) and 0.2 °C (7 data points). This is remarkable because the soil temperature was always lower than $T_{water,\,0}$, which means that the drinking water temperature increased along the pipe length although the soil was cooler. Two potential explanations are considered:

1. The drinking water temperature did not actually increase, but there is a measurement error. The measurement uncertainty (0.2 °C) is large compared to the measured temperature differences (0.1–0.2 °C). As so few data points show this effect, this explanation seems likely, and it demonstrates that the measurement uncertainty needs to be considered.
2. The soil temperatures were actually higher at these points, indicating that the modeled $T_{boundary}$ is incorrect (Table A5 shows a sensitivity to $T_{boundary}$). However, as these points were clustered in time, this explanation seems unlikely.

Figure A4 shows that the uncertainty for some measurements is quite large, especially for the tests at very short residence times (tests for 1 and 2 h); the uncertainty appears to be smaller at higher residence times. Two explanations are considered:

3. This is a coincidence. The size of the uncertainty in ΔTN correlates with the driving force ($T_{boundary} - T_{water,\,0}$) and is expected to be independent of the residence time τ. It seems likely that it is just a coincidence that the driving force was relatively small during the tests with small residence times. Before the controlled residence times tests started and data were already recorded, there were some days where $T_{water}(t) \approx T_{water,\,0}$), while $T_{boundary}$ and the temperature of the drinking water at the PS were different.
4. There is in fact a correlation between τ and $T_{boundary} - T_{water,\,0}$. The soil temperatures that we considered as $T_{boundary}$ may not be correct for all test conditions, i.e., the boundary condition cannot be retrieved from the STM+. The high flow tests (short residence times)

lasted relatively shortly (5 to 10 h) and the assumption of an (dynamic) equilibrium may not be valid, whereas it may be valid for the longer tests (at lower flows).
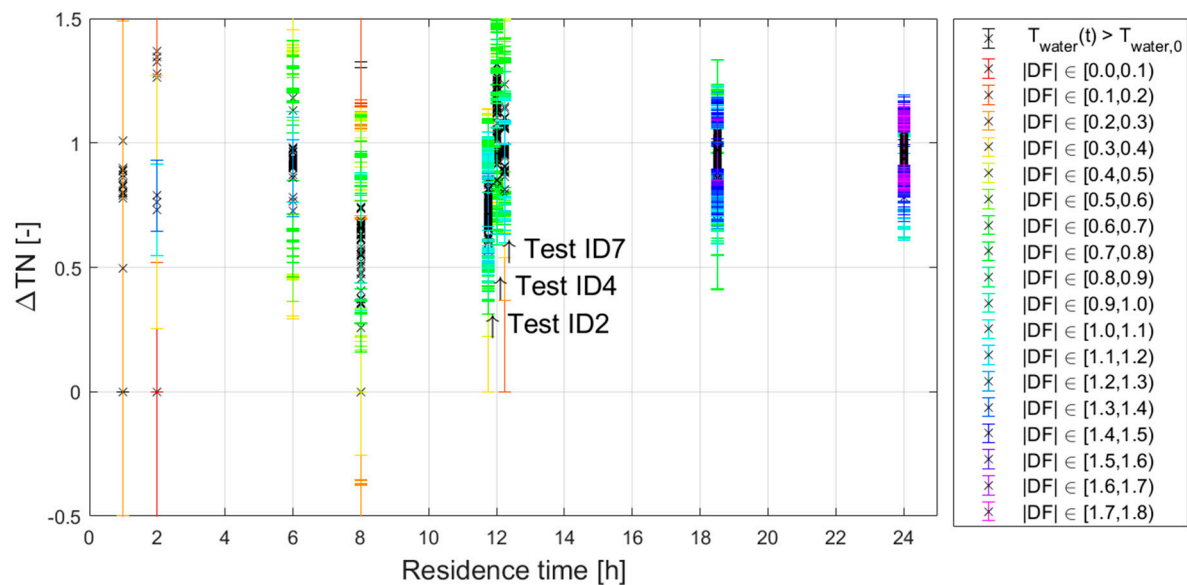
Figure A4. ΔTN versus residence time, individual data points (x) with corresponding uncertainty bars. Colors indicated the size of the driving force (DF = $T_{boundary} - T_{water,\,0}$); in black, negative DF; the size of uncertainty bars is equal to 0.2/DF. N.B. Tests ID2, 4, and 7 are conducted at 12 h, but, for readability, are plotted at around 12 h (indicated by the arrows).

Some data were filtered out:

- The 22 data points with a negative driving force are excluded from the validation.
- ΔTN is expected to be between 0 and 1. A data point with an uncertainty of $\overline{E} > 0.5$ is considered unreliable. These are data points for which the difference between $T_{water,0}$ and $T_{boundary}$ are small and therefore the value of ΔTN loses its meaning. There are 93 data points with $\overline{E} > 0.5$ (indicated with red and yellow error bars in Figure A4). These are excluded from the validation.

Figure A4 shows that some data points are larger than 1, and some of the data points including the uncertainty are smaller than 0. This should not be possible if the concept of the WTM+ is correct. It can be explained if the measured temperature differences are not correct. For this reason, the filtering step makes sense. Another explanation would be that the temperature difference between $T_{water,0}$ and $T_{boundary}$ is incorrect, which could be caused by measurement uncertainties (basically covered by the filtering step) or model uncertainties, i.e., $T_{boundary}$ is incorrect. Note that the timing of the (shift in) $T_{boundary}$ may lead to an error. For test 3, e.g., the residence time between L1 and L3 is 24 h, and the $T_{boundary}$ that is being applied is the one at 12 h from L1. In this particular case, the first 12 h $T_{boundary}$ will be an overestimate of the real boundary conditions, and the last 12 h will be an underestimate.

As a last step, the individual data points with similar residence times were grouped and shown in boxplots. The measurements at residence times of 1 and 2 h (tests 5 and 6, Table A3) have only a few data points and even fewer were left after filtering data points with high uncertainty in ΔTN. For the remaining tests, it appears that the variability between data points is in the same order of magnitude as the uncertainty per data point. Therefore, in the validation, the uncertainty in ΔTN will not be explicitly shown.

Table A3. An overview of the number of data points. Between brackets, the number of data points after filtering out measurements with high uncertainty.

ID	Start Time	End Time	Residence Time [h]	Amount of Data Points after Adjusting for Residence Time (and Filtering)
1	19 May 6:30	20 May 16:00	8.0	103 (60)
2	20 May 16:15	22 May 12:30	12.0	130 (128)
3	22 May 13:00	25 May 16:30	24.0	207 (207)
4	25 May 16:45	27 May 08:30	12.0	112 (109)
5	27 May 09:15	27 May 20:00	1.0	41 (0)
6	28 May 08:00	28 May 15:00	2.0	21 (2)
7	28 May 15:30	29 May 18:45	12.0	62 (57)
8	29 May 19:00	2 Jun 07:45	18.6	266 (266)
9	2 Jun 08:15	3 Jun 10:00	6.0	83 (41) [1]

Note: [1] The model results were only provided up to 3 June 2020 0:00. Therefore, the last 40 data points of measurements were not used.

Appendix B.3. Sensitivity Analysis of WTM+, Applied to a Single Pipe

For a single pipe, the sensitivity analysis for ΔTN was conducted analytically. The parameters in Equation (2) are kept constant; one by one, the parameters were multiplied with a factor of two or one-half, and the effect on ΔTN and the time it takes before $\Delta TN = 0.999$ were calculated. For example, halving D_1 means that ΔTN increases from 0.52 to 0.84 (multiplication factor of 1.63), and the time taken to reach $\Delta TN = 0.999$ decreases from 23.7 to 9.4 h (multiplication factor of 0.4). The higher the first value or the lower the second value, the more sensitive the model is toward this parameter. Table A4 shows that $\left(T_{boundary} - T_{water,0}\right)$, D_1, and λ_{soil} have the largest influence on ΔTN and the time taken to reach 0.999. ΔTN is not sensitive to the flow velocity in the turbulent regime (Nu, but this is especially true for the case of a thermal insulating pipe material and $D_3 > D_2$). It should be noted that, for the selected pipe diameter, residence time is only important if it is less than 24 h, which includes both laminar and turbulent flow regimes. For the other parameters, ΔTN is sensitive to them to a limited degree.

Table A4. The results of the sensitivity analysis with factor 2 variation in parameter values ($\rho_{water} = 1000$ kgm^{-3}, $C_{p,water} = 4.19$ Jkg^{-1}K^{-1}, $\lambda_{water} = 0.57$ Wm^{-1}K^{-1}), evaluated at $\tau = 2.5$ h, $\Delta TN \approx 0.5$. Table is sorted by 5th column.

Parameter	[Unit]	Default Value	Multiplication Factor	Resulting Multiplication Factor for ΔTN	Resulting Multiplication Factor for τ at Which $\Delta TN = 0.999$
$T_{boundary} - T_{water,0}$	[K]	5	2	2.00	1.00
D_1	[mm]	152	0.5	1.63	0.40
λ_{soil}	[Wm^{-1}K^{-1}]	1.60	2	1.62	0.40
t	[s]	9000	2	1.58	-
TSoI $\times D_1$	[m]	0.152	0.5	1.35	0.61
λ_{pipe}	[Wm^{-1}K^{-1}]	0.16	2	1.18	0.78
d_{pipe}	[mm]	4	0.5	1.11	0.86
Nu	[-]	100	2	1.01	0.98

Table A5 shows the results for the sensitivity analysis with more realistic parameter variations, for example, when flows and residence times are not known exactly, when a mistake is made in pipe diameter, pipe wall thickness, or pipe material, or when another soil type is present. In (the Dutch) practice D_1, d_{pipe}, and λ_{pipe} are typically well known. This shows that λ_{soil} is an important parameter. In this table, TSoI is not shown; this parameter is the unknown that we hope to estimate from the measurements. This shows that ΔTN is not sensitive to the flow velocity in the turbulent regime (Nu), but there is a big influence from turbulent to laminar flows.

Table A5. The results of the sensitivity analysis with realistic uncertainty in parameter values (ρ_{water} = 1000 kgm^{-3}, $C_{p,water}$ = 4.19 Jkg^{-1}K^{-1}, λ_{water} = 0.57 Wm^{-1}K^{-1}), evaluated at τ = 2.5 h, $\Delta TN \approx 0.5$. Table is sorted by 5th column.

Parameter	[Unit]	Default Value	Realistic Alternative	Explanation	Resulting Multiplication Factor for ΔTN	Resulting Multiplication Factor for τ at Which ΔTN = 0.999
Nu	[-]	100	3.66	laminar flow (i.so. turbulent)	0.61 (1/0.61 = 1.64)	1.90 (1/1.90 = 0.52)
			400	Q: 0.1 to 0.7 m/s	1.02	0.97
λ_{soil}	[Wm^{-1}K^{-1}]	1.60	1.9	wet sand (i.so. dry sand)	1.34	0.62
D_1	[mm]	152	125	one step down in nominal diameter	1.18	0.77
λ_{pipe}	[Wm^{-1}K^{-1}]	0.16	0.4	PE (i.so. PVC)	1.18	0.78
d_{pipe}	[mm]	4	3	one step down in pressure class	1.05	0.93
t	[s]	9000	10,000	measurement inaccuracy (ca. 15 min)	1.12	-
$T_{boundary} - T_{water,0}$	[K]	5	4.8	measurement inaccuracy (0.2 K)	1.04	1.00

Appendix B.4. Extra Results for Case Study 1

Figure A5 shows ΔTN versus residence time with the measurement in boxplots and theoretical lines for various values of TSoI, for the case where $T_{boundary}$ was taken from the STM+ passive mode.
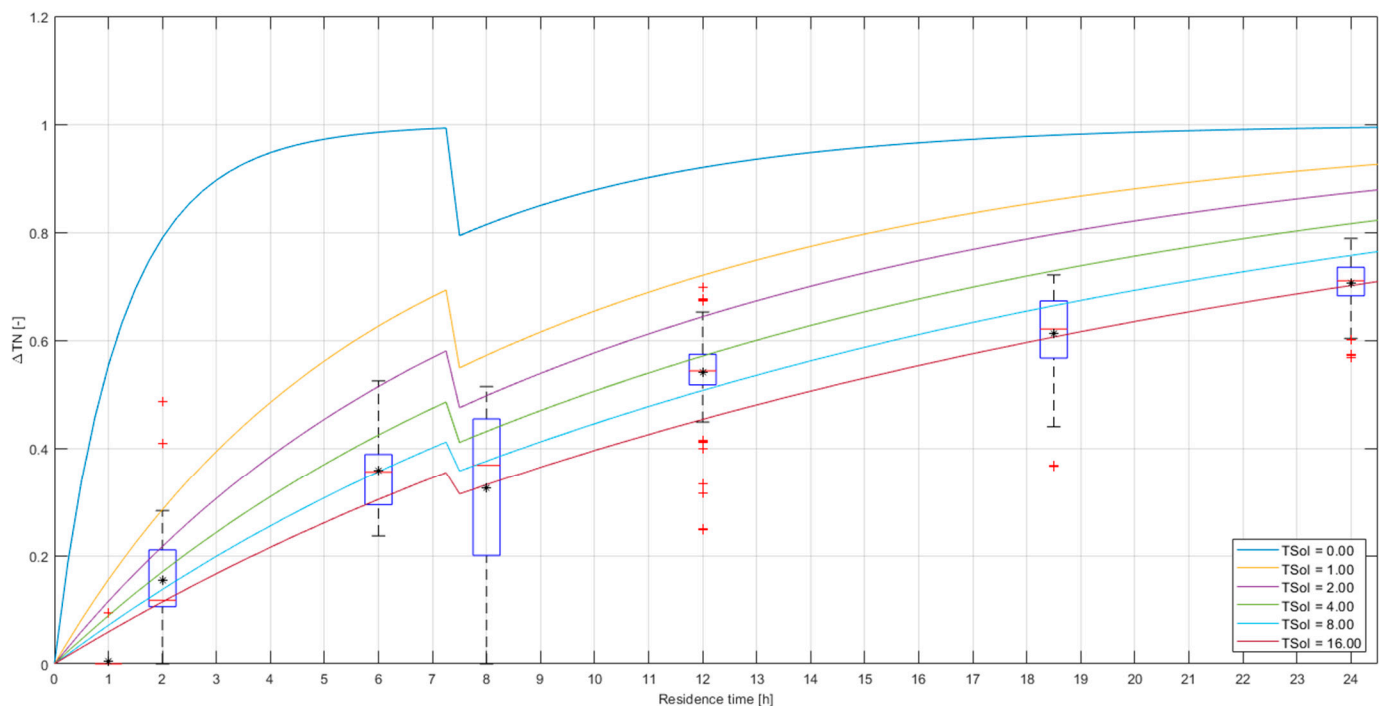
Figure A5. ΔTN versus residence time, with $T_{boundary}$ from STM+ passive mode. Measured data are in boxplots, where the box represents the data between the 25th and 75th percentiles, the central red lines indicate the median, and the black star indicates the average. The whiskers extend to the most extreme data points not considered outliers, and the outliers are plotted as red plus symbols. The curves represent Equation (4), with different values for the TSoI. The threshold for turbulent flows is determined at Re = 5000. Data points (22) with ΔTN < 0 are discarded. Data points (1) with E $\geq$ 0.5 are discarded.

Appendix C. Case Study 2

Appendix C.1. Additional Information on Case Study 2: Soil Temperatures

The local circumstances that influence the soil temperature around the pipes are determined by the pipe installation depth, soil type, soil cover, and local anthropogenic heat sources. Specifically, for the Almere DWDN, the following are found:

- There is a variation in installation depth with the top of the distribution mains in the older parts (built between 1980 and 2000, roughly the center and southern part, amongst which areas A and D in Figure 3) at −1.3 m and in the newer parts (roughly the western and north-eastern part, amongst which areas B, E, and C in Figure 3) at −1.1 m (meaning that the center of the Ø110 and Ø160 mm pipes are installed at −1.35 to −1.38 m and −1.15 to −1.18 m, respectively). The transport mains (>180 mm) are installed at ca. 1.5 m coverage (center of the Ø200 and Ø310 mm pipe at ca. −1.6 to −1.7 m).
- The soil type is influenced by the backfill that was used for pipe installation. The older parts have a mixture of sand and clay, and the newer parts have sand only.
- The variation in soil cover (asphalt, tiles, grass, or bushes) is very high and very distributed over the entire area. There is even soil cover variation over the length of a single pipe. This level of detail was not considered in this study.
- Above-ground anthropogenic heat sources were not considered either. It is not yet entirely clear which are important and how much influence they would have.
- Below-ground anthropogenic heat sources include electricity cables and the DHN, where the DHN most likely has a significant effect [17]. The northwestern part of Almere (amongst which areas A and C; see Figure 3) has a DHN. The effect of the DHN parallel to the DWN is not considered in this paper as the distance between the two is more than 2.5 m. The crossings of DWDN and DHN pipes are taken into consideration.

The areas with pipes at −1.35 m and with a clay and sand mixture backfill roughly overlap, and the areas with pipes at −1.15 m and with a sand backfill also roughly overlap. This means that there are transport mains with and without DHN crossings, distribution mains in the older parts of the network with and without DHN crossings, and distribution mains in the newer parts of the network (only without DHN crossings).

For these five subgroups of pipes, a specific value of $T_{boundary}$ was determined for 31 August 2020. The parameters of Equation (1) are determined as follows:

- τ: the residence time follows from the hydraulic network model. Here, the demand patterns of 31 August 2020 were applied, but the model was not calibrated for this particular day, so there may be some valve positions that are incorrect, which may lead to errors in residence time.
- $T_{boundary}$: $T_{boundary}$ was estimated by using weather data, processed with the STM [4,18] and STM+ [17]. There were no soil temperature measurements available. Five different boundary conditions were suggested (Table A7):

  a. T_{TM} is the soil temperature around transport mains (D ≥ 180 mm). T_{TM} = 18.0 °C. This is the STM calculated temperature at −1.7 m (Figure A6) in peri-urban areas (clay/sand under grass).

  b. T_{TM_DHN} is the soil temperature around transport mains with a DHN crossing. T_{TM_DHN} = 20.1 °C. This is the STM calculated temperature at −1.7 m in peri-urban areas (clay/sand under grass) + 2.1 °C from the primary network DHN as from the STM+.

  c. T_{TM} is the soil temperature around distribution mains in the older part of Almere. T_{DM} = 18.7 °C. This is the STM calculated temperature at −1.35 m (Figure A6) in peri-urban areas (clay/sand under grass).

  d. T_{TM} is the soil temperature around distribution mains with a DHN crossing in the older part of Almere. T_{DM_DHN} = 19.5 °C. This is the STM calculated temperature at −1.35 m in peri-urban areas (clay/sand under grass) + 0.8 °C from the secondary network DHN as from the STM+.

  e. T_{TM_NE} is the soil temperature around distribution mains in the newer (north-eastern) part of Almere. T_{DM_NE} = 20.5 °C. This is the maximum drinking water temperature that was measured in area B (Figure 3) and is the average of the STM calculated temperatures at −1.15 m (Figure A6) for peri-urban (clay/sand under grass) and urban (sand, under tiles with various shade conditions) areas.

- $T_{water,0}$: drinking water temperature measured at locations F1 and F2 (13.7 and 13.3 °C, respectively).
- $T_{water}(\tau)$: drinking water temperature measured at hydrants (Figure 3).
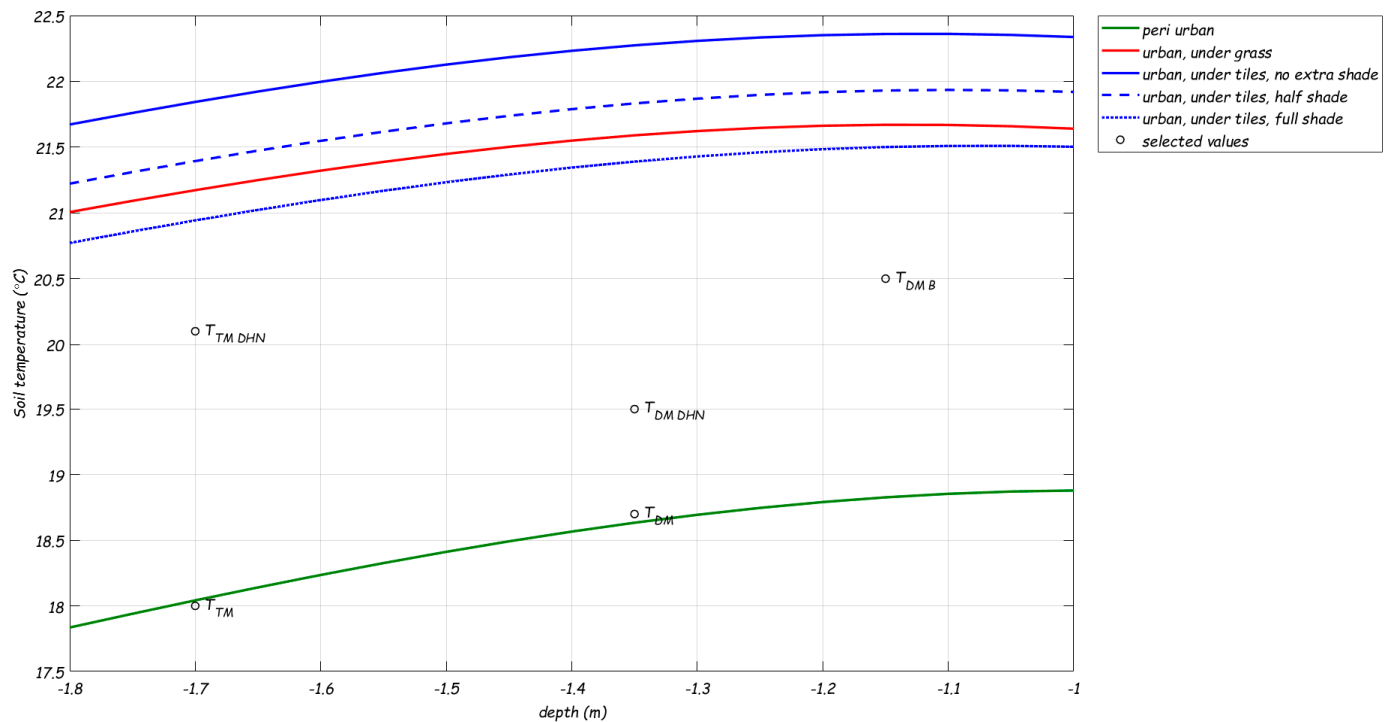
Figure A6. The modeled soil temperature (STM) at various depths for 31 August 2020. Indicated are temperatures around transport mains (T_{TM}), transport mains with crossing of DHN ($T_{TM\,DHN}$), distribution mains in most of Almere (T_{DM}), distribution mains with crossing of DHN ($T_{DM\,DHN}$), distribution mains in area B ($T_{DM\,B}$).

Table A6. The settings of STM [5] where weather input data were used from Schiphol airport (20 km from Almere).

Scenario	λ_{soil}	ρ_{soil}	$C_{p,\,soil}$	α_{soil}	Cover	Albedo	Global Radiation	QF	$a3$
	$W\cdot m\cdot K^{-1}$	$kg\cdot m^{-3}$	$J\cdot kg^{-1}\cdot K^{-1}$	10^{-6} $m^2 s^{-1}$		-	$W\cdot m^{-2}$	$W\cdot m^{-2}$	$W\cdot m^{-2}$
Peri-urban, under grass (clay)	1.0	2.10^3	1.10^3	0.5	Grass	0.12	R_g	50	−50
Urban, under grass (sand)	1.2	2.10^3	1.10^3	0.6	Grass	0.12	R_g	100	−100
Urban, under tiles, no extra shade (sand)							R_g		
Urban, under tiles, half shade (sand)	1.2	2.10^3	1.10^3	0.6	Tiles	0.12	$50\% \times R_g$	100	−100
Urban, under tiles, full shade (sand)							0		

Table A7. The values of $T_{boundary}$ for the Almere DWDN.

$T_{boundary}$	Value	Pipe Group Conditions	Where in Network	Where in Model
T_{TM}	18.0 °C.	−1.5 m, sand + clay, no DHN crossings	Most transport mains (>180 mm)	
$T_{TM\,DHN}$	T_{TM} + 2.1 = 20.1 °C.	−1.5 m, sand + clay, with DHN crossings	Some transport mains (>180 mm) with crossings of DHN	
T_{DM}	18.7 °C.	−1.3 m, sand + clay, no DHN crossings	Area A and D	distribution mains in whole network, except area B
$T_{DM\,DHN}$	T_{DM} + 0.8 = 19.5 °C.	−1.3 m, sand + clay, with DHN crossings	Part of Area A with crossings of DHN	distribution mains in whole network, except area B
$T_{DM\,NE}$	20.5 °C.	−1.1 m, sand, no DHN crossings	Area B, C, and E	distribution mains in area B

Appendix C.2. Additional Information on Case Study 2: WTM+

The hydraulic model of the area (provided by Vitens) is characterized by 21054 nodes and 21,987 pipes. To simulate the drinking water temperature in this network, the WTM+ (Equations (1) and (2)) was integrated into an Epanet-MSX model. Epanet-MSX requires some general settings (a fifth-order Runge–Kutta integrator was used as solver, the hydraulic model was used to evaluate 72 h, and results are saved and analyzed for the last 24 h) and case-specific settings (Table A8).

Table A8. The parameter values of Equation (2) and (4) for case 2. Constants for water are used (ρ_{water} = 1000 kgm^{-3}, $C_{p,water}$ = 4.19 Jkg^{-1}K^{-1}, λ_{water} = 0.57 Wm^{-1}K^{-1}, α_{water} = 0.14 m^{2}s^{-1}).

Parameter	Unit	Value	Uncertainty	Reference
D_1	mm	50–300	-	Hydraulic network model Almere, from Vitens
D_2	mm	$1.052 \times D_1$	-	Outside diameter of PVC estimated with multiplication factor to inside diameter. AC pipes treated as PVC.
λ_{pipe}	Wm^{-1}K^{-1}	0.16	Some pipes are AC, but modeled as PVC	AC pipes treated as PVC [4]
Nu	-		Unclear where transition between turbulent and laminar flow is, transition at Re = 5000 from case study 1	For Re > 5000: Nu = 0.027 $Re^{0.8}$ $Pr^{0.33}$ [4], Re from hydraulic network model Almere, Pr = 7. For Re <= 5000 Nu = 3.66
D_3	mm	D_2 + TSoI $\times D_1$	Unknown	To be determined
λ_{soil}	Wm^{-1}K^{-1}	1.6	Unknown	Dry sand [17]
$T_{water,0}$	°C	$T_{water,F1}$= 13.7 $T_{water,F2}$= 13.3	± 0.05 °C	Vitens
T_{water}	°C	13.0–21.0	± 0.05 °C	Measured at hydrants, Vitens
$T_{boundary}$	°C	T_{DM} = 18.7 T_{DM_DHN} = 19.5 T_{DM_NE} = 20.5 T_{TM} = 18 T_{TM_DHN} = 20.1	Unknown	For stagnant water, from STM (Table A7).

Appendix C.3. Sensitivity Analysis of WTM+, Applied to a Drinking Water Distribution Network

The sensitivity analysis of the single pipe is insightful. However, in a network with a variety of pipe diameters and topologies, residence times in the different types of pipes (e.g., transport and distribution mains of different lengths) will vary. Executing an effective sensitivity study of the drinking water temperature at household connections in a DWDN is

not straightforward. Therefore, a limited sensitivity analysis is conducted for case study 2, where we only focus on the most important parameters, as they follow from the previous section, namely TSoI, $T_{boundary}$, and λ_{soil}. Pipe length and pipe diameter were added.

Five areas (A–E) were selected for the sensitivity analysis. The areas differ in surrounding soil temperatures and residence times from the sources. Area A and B have comparable residence times from the sources (Table A9). Area C is far from the reservoir, with a large residence time. Area D is the oldest neighborhood (built in the 1980s) and has an older design philosophy (larger diameters, more looped than area A and B). Area E is very close to the reservoir (see Figure 3). A DHN is installed next to the DWDN in areas A and C, but not in areas B, D, and E.

Table A9. The residence times of study areas in the Almere DWDN.

	$T_{water,0}$	Residence Time (h)	Conditions for $T_{boundary}$
A	13.3	5–15	T_{DM}, T_{DM_DHN}
B	13.7	10–15	T_{DM_NE}
C	13.3	>24	T_{DM}, T_{DM_DHN}
D	13.3	>10	T_{DM}
E	13.7	10–15	T_{DM_NE}

The parameter values for the base case are best guesses from a priori knowledge of the area; see Appendix C.3. This case serves as a reference for the sensitivity analysis. In the sensitivity analysis, the TSoI was varied between 0.1 and 10. To test the sensitivity to the soil temperature, $T_{boundary}$ was specified in various scenarios for the five subgroups of pipes (i.e., transport mains with and without DHN crossings, distribution mains with and without DHN crossings, and distribution mains in the north–east without DHN crossings). For λ_{soil}, a range from 1.1 to 1.9 Wm^{-1}K^{-1} was used. To test the effect of street lengths, the pipe length was increased and decreased by 10%; to test the effect of different design philosophies, the pipe diameter was increased and decreased by 10% (Table A10). Furthermore, the areas A–E were analyzed separately to identify the effect of network layout and residence time from the reservoirs.

Table A10. The settings for the sensitivity analysis. Blanks are equal to the base case. Other parameter values are in Table A8.

Scenario	Scale %	TSoI	λ_{soil} Wm^{-1}K^{-1}	T_{DM} °C	T_{DM_DHN} °C	T_{DM_NE} °C	T_{TM} °C	T_{TM_DHN} °C
Base		1	1.6	18.7	19.5	20.5	18.0	20.1
TSoI		0.1–10						
$T_{boundary,1}$				14.7–23.1	T_{DM} + 0.8		T_{DM}–0.5	T_{DM} + 1.4
$T_{boundary,2}$						15.0–23.0		
$T_{boundary,3}$							13.7–24.2	
$T_{boundary,4}$					13.7–24.2			
$T_{boundary,5}$								13–23
λ_{soil}			1.1–1.9					
D_1	−10 to +10							
Pipe length	−10 to +10							

For all scenarios, the drinking water temperature (T_{water}) was determined at all time steps (*t*) at all non-zero demand nodes (*n*). All scenario results were compared to the base case (Tables A8 and A10), i.e., the temperature difference ($\Delta T(t,n) = T_{water,base}(t, n) - T_{water,scenario}(t,n)$) was calculated. Next, the average of ΔT over all time steps and all nodes was calculated for each area (A–E) separately, plus for the total network. Note that ΔT can be negative or positive.

The sensitivity analysis shows the following:

- TSoI: Figure A7a shows that $\Delta T \leq 0.8$ °C for a TSoI < 1. The larger the TSoI, the slower the heat exchange between soil and drinking water, and, in this case, it means that, at a larger TSoI, T_{water} will be lower. Figure A7a shows that the effect is similar for most

areas but stronger in area B. This is most likely caused by a difference in residence times. The residence times toward area C, e.g., are large (>20 h) and thus most likely the drinking water temperature at most nodes has reached $T_{boundary}$, even with an extra delay due to the TSoI, leading to a maximum of $\Delta T = 0.8$ °C. On the other hand, areas B and E are very close to a reservoir, and the effect of a larger TSoI is more noticeable ($\Delta T \geq 1.2$ °C).
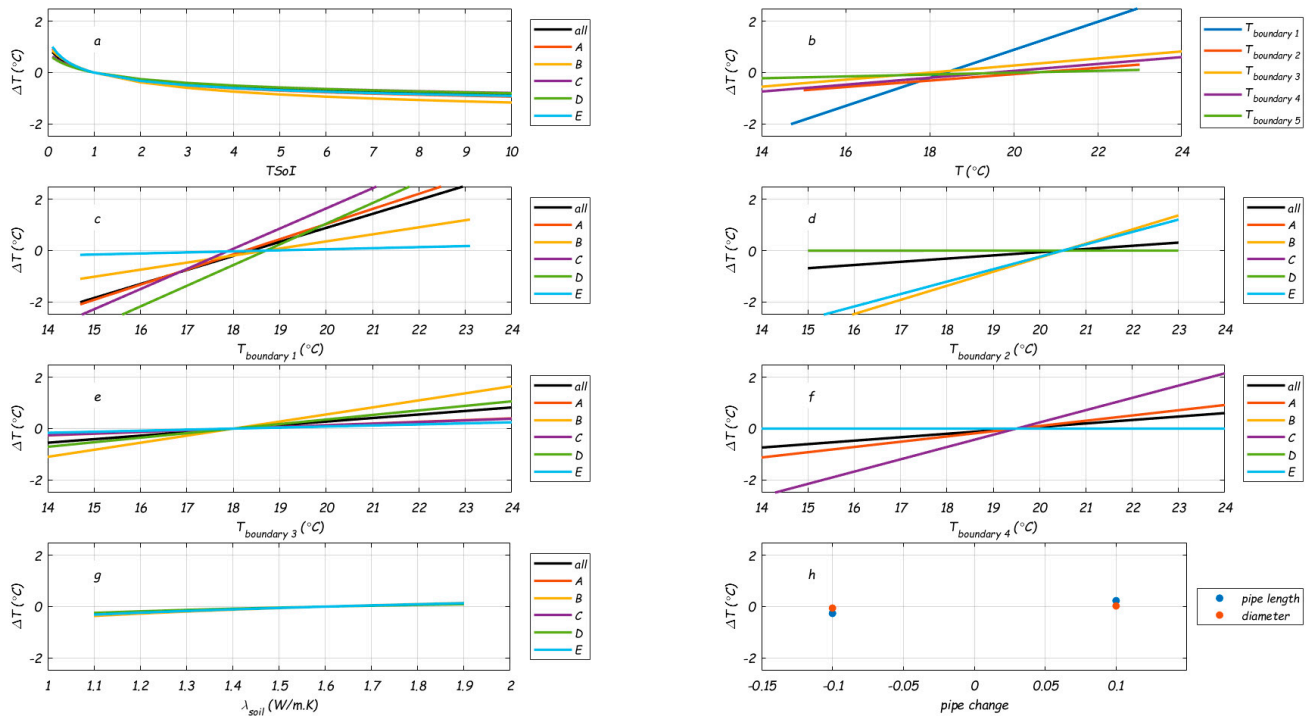
Figure A7. The sensitivity analysis results. In each figure, curves A to E give the average (across all nodes and timesteps in a separate area of the network A to E) difference in modeled temperatures (compared to the modeled temperature of base scenario) due to a variation in (**a**) TSoI, (**b**–**f**) T_{wall}, (**g**) λ_{soil}, (**h**) pipe length and diameter.

a. $T_{boundary}$: the model is very sensitive to $T_{boundary}$. Especially scenario $T_{boundary,1}$ shows a large effect; the other scenarios have a more local effect, and the effect is smaller (Figure A7b). The larger the area where this local $T_{boundary}$ is imposed, the larger the number of customers nodes that are affected.

b. The $T_{boundary,1}$ scenario shows that, when $T_{boundary}$ decreases or increases at (almost) all locations (Figure A7c), the T_{water} changes with it. The effect is small (but not zero) in areas B and E, where $T_{boundary}$ is the same as in the base case.

c. The $T_{boundary,2}$ scenario shows the local effect of T_{DM_NE} only in the areas that have this boundary condition (Area B and E); there is no effect in areas A, C, and D. A range of 8 °C (from 15 to 23 °C) in T_{DM_NE} leads to a range of 5 °C (-2.5 to 1.5 °C) in ΔT and thus in T_{water} in areas B and E (Figure A7d).

d. The $T_{boundary,3}$ scenario (Figure A7e) shows the effect when only $T_{boundary}$ around transport mains is changed. An 8 °C change in $T_{boundary}$ leads to a ca. 1.5 °C change in T_{water}.

e. The $T_{boundary,4}$ scenario (Figure A7f) shows that a different $T_{boundary}$ at DHN crossings with the distribution mains has a small effect, but larger than 0 °C. This effect is more apparent when we only look at the areas that have distribution mains with DHN crossings (areas A and C), where the effect is larger in area C (an 8 °C change in $T_{boundary}$ leads to a ca. 5 °C change in T_{water}) with longer residence times than in area A. In area A, the effect is also noticeable and should not be neglected.

- The $T_{boundary,5}$ scenario (Figure A7b) only considers the crossings of the DHN with transport mains. The effect is almost 0 ($<\pm 0.2\ ^\circ$C). This means that the current number of DHN crossings with the transport mains does not lead to higher T_{water}.
- λ_{soil}: the ΔT due to variations in λ_{soil} is less than $\pm 0.3\ ^\circ$C (Figure A7g), and this means that λ_{soil} is not the most important parameter to estimate accurately for the WTM+ in a real DWDN. It should be noted that $T_{boundary}$, as estimated with the STM, is indeed sensitive to λ_{soil}.
- Pipe length and diameter: the ΔT is less than $\pm\ 0.15\ ^\circ$C for pipe length and diameter changes (Figure A7h); the WTM+ is not very sensitive to these parameters. This means that, when the WTM+ is applied to the DWDN of case study 2, the results will be representative for a range of DWDNs throughout the Netherlands and the five areas are representative for the effects of differences in residence time, local $T_{boundary}$, and network layouts.

Appendix C.4. Extra Results for Case Study 2

For the extra cases, the TSoI was varied between 0.1 and 1 in steps of 0.1, and between 1 and 10 in steps of 1, meaning that 19 different TSoI values were simulated. $T_{boundary}$ was varied for area A (resp. area B) between 18.0 and 21.0 °C (19.0 and 22.0 °C) in steps of 0.1 °C, meaning that 30 different $T_{boundary}$ values were considered for both areas A and B separately. The combination of the two would mean $19 \times 30 \times 30 = 17{,}100$ simulations. To save simulation time, 19 simulations were run for a specific $T_{boundary}$ and varying TSoI. Then, the resulting $T_{water}(\tau)$ at the measurement locations was converted to $T^*_{water}(\tau)$ for the varying $T_{boundary}$ values by substituting them into Equation (3).

$$T^*_{water}(\tau) = T^*_{boundary} + \left(T_{water,0} - T^*_{boundary}\right) \left(\frac{\left(T_{water}(\tau) - T_{boundary}\right)}{\left(T_{water,0} - T_{boundary}\right)} \right) \tag{A11}$$

where, for area A (resp. area B), $T_{water,0} = 13.7\ ^\circ$C (13.3 °C) and $T_{boundary} = 20.5\ ^\circ$C (19.5 °C), and $T^*_{boundary}$ = 18.0–21.0 °C (19.0–22.0 °C). Note that, in Equation (A11), the boundary conditions are not time-dependent as they are in case study 1. This approach calculates the value for τ from the modeled temperatures instead of using them directly from the hydraulic network model. Note that the results are not as accurate as a new simulation would be as $T_{boundary}$ was assumed to be a single value instead of changing between pumping station and measurement location, with a variable residence time in pipes with different diameters.

Compared to the base case, a larger TSoI (>1) will lead to a slower change in the drinking water temperature. There will be locations where T_{water} will not yet have reached $T_{boundary}$, which will result in a lower T_{water} than at TSoI = 1. There will also be locations that have relatively high residence times and T_{water} will have reached $T_{boundary}$, which means that T_{water} will be the same as in the base case. A larger $T_{boundary}$ will lead to an increase in all modeled drinking water temperatures, with the largest effect in absolute terms at the locations with higher residence times. This means that a change in TSoI mostly affects the temperatures at lower residence times, and a change in $T_{boundary}$ mostly affects the temperatures at higher residence times. When both parameters are changed simultaneously, the parameter leading to the smallest error with respect to the measurements can be found. Figure A8a illustrates the effect of changing TSOI compared to the base case. It shows that most cyan points (TSoI = 2) are lower than the magenta points (TSoI = 1), and the difference is much smaller near $T_{modeled} = 20.5\ ^\circ$C (which is the maximum) than, e.g., at $T_{modeled} = 17\ ^\circ$C. Figure A8b illustrates the effect of changing $T_{boundary}$ compared to the base case. It shows that lowering $T_{boundary}$ (cyan points experience a $T_{boundary} = 0.5\ ^\circ$C lower than the magenta points) leads to lower temperatures for all locations, but most distinctively for the locations with higher temperatures.
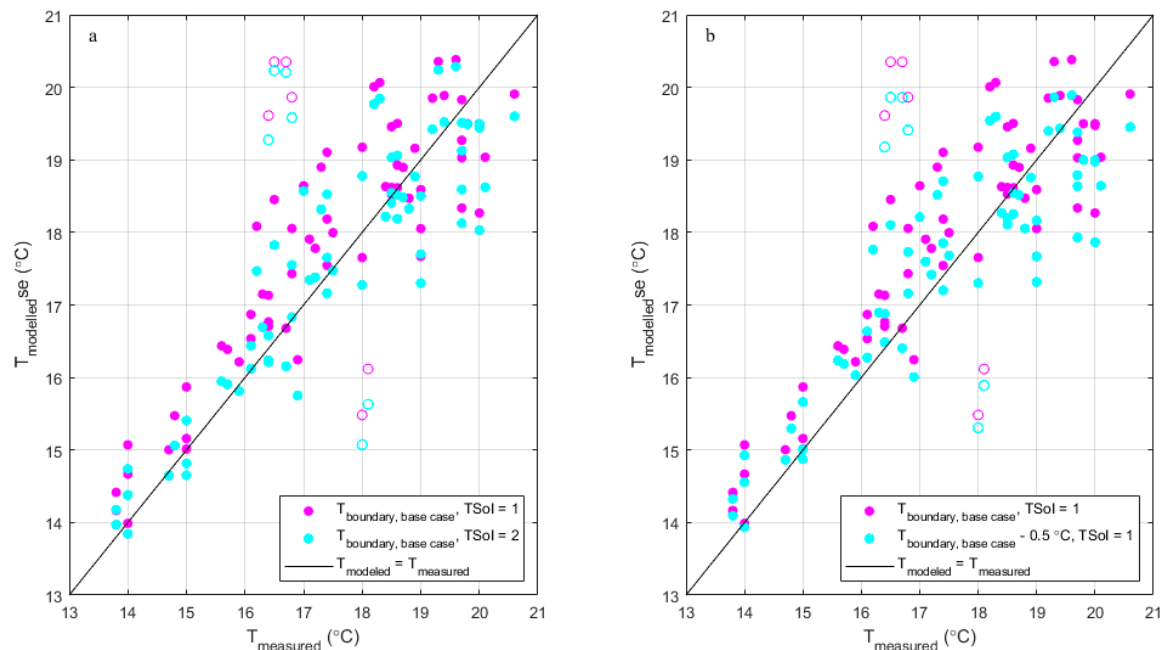
Figure A8. The validation of WTM+; model results compared to field measurements for (**a**) the base case ($T_{boundary}$ = 19.5 and 20.5 °C for area A and area B, respectively) at TSoI = 1 and TSoI = 2, and (**b**) the extra case with adjusted $T_{boundary}$ = 18.5 and 19.5 °C for area A and area B, respectively.

Figure A9 shows the RMSE and R² as a function of the TSoI for $T_{boundary}$ as in the base case (this is the same as the TSoI scenario in Appendix C.3). The RMSE decreases from 1.5 °C (without outliers) to 0.76 °C with an increase in the TSoI from 0.05 to 2, and then increases again for TSoI > 2. At the same time, the R² increases from <0 (without outliers) to 0.80, and then decreases. For the combination of areas A and B, there appears to be an optimum at TSoI = 2, with the values for $T_{boundary}$ as in the base case. For area A, resp. area B, by themselves, there appears to be an optimum at TSoI = 1, resp. TSoI = 3, with the base case values for $T_{boundary}$. The same exercise has been repeated with an adjusted $T^*_{boundary}$ for the extra cases. Table A11 gives the goodness of fit parameters.
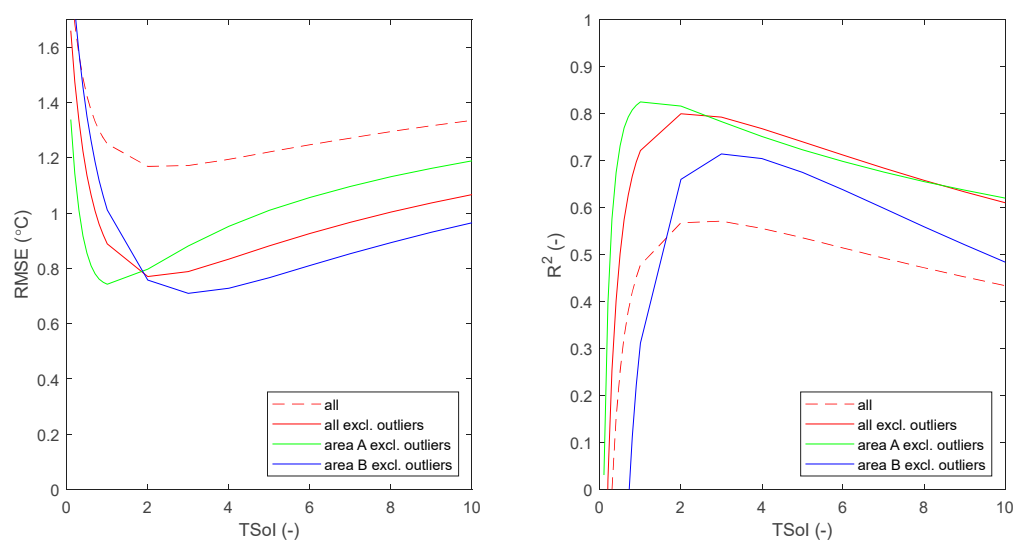
Figure A9. The RMSE (**left**) and R² (**right**) for the modeled data compared to the measured data for various values of TSoI, for all measurements, including (red dotted line) and excluding outliers (red full line), and the areas A (green) and B (blue) without the outliers.

Table A11. The goodness of fit parameters for the base case, best fit base case (best TSoI), and best fit extra cases (combination of best fit TSoI and $T_{boundary}$).

Figure, Line Color	Area	Case	$T_{boundary}$ (°C)	TSoI	Excluding Outliers		Including Outliers	
					RMSE (°C)	R^2	RMSE (°C)	R^2
Figure 7a, red	A	Base	19.5	1	0.75	0.82	0.92	0.72
Figure 7a , blue	B	Base	20.5	1	1.01	0.31	1.49	0
Figure A8a,b, magenta	Total	Base	19.5/20.5	1	0.92	0.72	1.25	0.48
n.a.	A	Change in TSoI	19.5	2	0.80	0.82	1.03	0.68
n.a.	B	Change in TSoI	20.5	2	0.76	0.66	1.29	0.08
Figure A8a, cyan	Total	Change in TSoI	19.5/20.5	2	0.77	0.80	1.17	0.57
n.a.	A	Change in $T_{boundary}$	19.0	1	0.88	0.71	1.06	0.56
n.a.	B	Change in $T_{boundary}$	20.0	1	0.80	0.50	1.24	0
Figure A8b, cyan	Total	Change in $T_{boundary}$	19.0/20.0	1	0.83	0.72	1.15	0.49
n.a.	A	Best fit TSoI	19.5	1	0.75	0.82	0.92	0.72
n.a.	B	Best fit TSoI	20.5	3	0.71	0.71	1.22	0.21
Figure A8a, cyan	Total	Best fit TSoI	19.5/20.5	2	0.77	0.80	1.17	0.57
Figure 7b, red	A	Optimal, best fit (RMSE) $T_{boundary}$ AND TSoI	20.1	2	0.70	0.88		
n.a.		Best fit (R^2) $T_{boundary}$ AND TSoI	20.5	3	0.74	0.89		
Figure 7b, blue	B	Optimal, best fit (RMSE) $T_{boundary}$ AND TSoI	20.1	2	0.70	0.67		
n.a.		best fit (R^2) $T_{boundary}$ AND TSoI	21.4	7	0.78	0.74		
n.a	Total	best fit (RMSE) $T_{boundary}$ AND TSoI	20.1	2	0.70	0.83		
n.a.		best fit (R^2) $T_{boundary}$ AND TSoI	20.5	3	0.72	0.84		

References

1. Calero Preciado, C.; Boxall, J.; Soria-Carrasco, V.; Martínez, S.; Douterelo, I. Implications of climate change: How does increased water temperature influence biofilm and water quality of chlorinated drinking water distribution systems? *Front. Microbiol.* **2021**, *12*, 658927. [CrossRef] [PubMed]

2. Ahmad, J.I.; Dignum, M.; Liu, G.; Medema, G.; van der Hoek, J.P. Changes in biofilm composition and microbial water quality in drinking water distribution systems by temperature increase induced through thermal energy recovery. *Environ. Res.* **2021**, *194*, 110648. [CrossRef] [PubMed]

3. Agudelo-Vera, C.; Avvedimento, S.; Boxall, J.; Creaco, E.; de Kater, H.; Di Nardo, A.; Djukic, A.; Douterelo, I.; Fish, K.E.; Iglesias Rey, P.L.; et al. Drinking Water Temperature around the Globe: Understanding, Policies, Challenges and Opportunities. *Water* **2020**, *12*, 1049. [CrossRef]

4. Blokker, E.J.M.; Pieterse-Quirijns, E.J. Modeling temperature in the drinking water distribution system. *J. Am. Water Work. Assoc.* **2013**, *105*, E19–E29, Erratum in *J. Am. Water Work. Assoc.* **2018**, *110*, 98. [CrossRef]

5. Agudelo-Vera, C.M.; Blokker, M.; de Kater, H.; Lafort, R. Identifying (subsurface) anthropogenic heat sources that influence temperature in the drinking water distribution system. *Drink. Water Eng. Sci.* **2017**, *10*, 83–91. [CrossRef]

6. Agudelo-Vera, C.M.; Blokker, E.J.M.; Pieterse-Quirijns, E.J. Early warning system to forecast maximum temperature in drinking water distribution systems. *J. Water Supply Res. Technol.—AQUA* **2015**, *64*, 496–503. [CrossRef]

7. De Pasquale, A.M.; Giostri, A.; Romano, M.C.; Chiesa, P.; Demeco, T.; Tani, S. District heating by drinking water heat pump: Modelling and energy analysis of a case study in the city of Milan. *Energy* **2017**, *118*, 246–263. [CrossRef]

8. Hubeck-Graudal, H.; Kirstein, J.K.; Ommen, T.; Rygaard, M.; Elmegaard, B. Drinking water supply as low-temperature source in the district heating system: A case study for the city of Copenhagen. *Energy* **2020**, *194*, 116773. [CrossRef]

9. Díaz, S.; Boxall, J.; Lamarche, L.; González, J. The impact of ground heat capacity on drinking water temperature. *J. Water Resour. Plan. Manag.* **2023**, *149*, 04023012. [CrossRef]

10. Hypolite, G.; Ferrasse, J.H.; Boutin, O.; Del Sole, S.; Cloarec, J.F. Dynamic modeling of water temperature and flow in large water system. *Appl. Therm. Eng.* **2021**, *196*, 117261. [CrossRef]

11. Jakubek, D.; Ocłoń, P.; Nowak-Ocłoń, M.; Sułowicz, M.; Varbanov, P.S.; Klemeš, J.J. Mathematical modelling and model validation of the heat losses in district heating networks. *Energy* **2023**, *267*, 126460. [CrossRef]
12. Hussein, A.; Klein, A. Modelling and validation of district heating networks using an urban simulation platform. *Appl. Therm. Eng.* **2021**, *187*, 116529. [CrossRef]
13. Danielewicz, J.; Śniechowska, B.; Sayegh, M.A.; Fidorów, N.; Jouhara, H. Three-dimensional numerical model of heat losses from district heating network pre-insulated pipes buried in the ground. *Energy* **2016**, *108*, 172–184. [CrossRef]
14. Wang, H.; Meng, H.; Zhu, T. New model for onsite heat loss state estimation of general district heating network with hourly measurements. *Energy Convers. Manag.* **2018**, *157*, 71–85. [CrossRef]
15. Kuntuarova, S.; Licklederer, T.; Huynh, T.; Zinsmeister, D.; Hamacher, T.; Perić, V. Design and Simulation of District Heating Networks: A Review of Modeling Approaches and Tools. *Energy* **2024**, *305*, 132189. [CrossRef]
16. Hägg, R. Dynamic Simulation of District Heating Networks in Dymola. Master's Thesis, Lund University, Lund, Sweden, 2016.
17. van Esch, J. *BTM+ Model and Expert Tool*; Deltares: Delft, The Netherlands, 2022.
18. Çengel, Y.A. *Heat Transfer: A Practical Approach*; McGraw-Hill Companies, Inc.: New York, NY, USA, 1998; 1006p.
19. Blokker, E.J.M.; van Osch, A.M.; Hogeveen, R.; Mudde, C. Thermal energy from drinking water and cost benefit analysis for an entire city. *J. Water Clim. Chang.* **2013**, *4*, 11–16. [CrossRef]
20. Shang, F.; Uber, J.G. *EPANET Multi-Species Extension User's Manual*; EPA: Cincinnati, OH, USA, 2008.
21. Trinh, K.T. On the critical Reynolds number for transition from laminar to turbulent flow. *arXiv* **2010**, arXiv:1007.0810.
22. Blokker, M.; van Summeren, J.; van Laarhoven, K. Measuring drinking water temperature changes in a distribution network. In Proceedings of the 2nd International Joint Conference WDSA/CCWI, Valencia, Spain, 18–22 July 2022.
23. Vewin and Energie-Nederland. *Intersectoral Agreement Drinking Water and District Heating Pipes: Agreements on Distances*; Vewin and Energie-Nederland: Den Haag, The Netherlands, 2024. (In Dutch)